Pergamon

Geochimica et Cosmochimica Acta, Vol. 68, No. 12, pp. 2659–2679, 2004
Copyright © 2004 Elsevier Ltd
Printed in the USA. All rights reserved
0016-7037/04 $30.00 + .00

doi:10.1016/j.gca.2003.12.002

Carbon isotope effects in carbonate systems

PETER DEINES*

Department of Geosciences, The Pennsylvania State University, University Park, PA 16802, USA

(*Received March* 4, 2002; *accepted in revised form December* 5, 2003)

Abstract—Global carbon cycle models require a complete understanding of the $\delta^{13}C$ variability of the Earth's C reservoirs as well as the C isotope effects in the transfer of the element among them. An assessment of $\delta^{13}C$ changes during CO_2 loss from degassing magmas requires knowledge of the melt-CO_2 carbon isotope fractionation. In order to examine the potential size of this effect for silicate melts of varying composition, ^{13}C reduced partition functions were computed in the temperature range 275 to 4000 K for carbonates of varying bond strengths (Mg, Fe, Mn, Sr, Ba, Pb, Zn, Cd, Li, and Na) and the polymorphs of calcite. For a given cation and a given pressure the ^{13}C content increases with the density of the carbonate structure. For a given structure the tendency to concentrate ^{13}C increases with pressure. The effect of pressure (‰/10 kbar) on the size of the reduced partition function of aragonite varies with temperature; in the pressure range 1 to 10^5 bars the change is given by:

$$\Delta^{13}C_{Paverage} = -0.01796 + 0.06635 * \frac{10^3}{T} + 0.006875 * \frac{10^6}{T^2} \quad (1)$$

For calcite III the pressure effect is on average 1.4× larger than that for aragonite at all temperatures. The nature of the cation in a given structure type has a significant effect on the carbon isotope fractionation properties. The tendency to concentrate ^{13}C declines in the series magnesite, aragonite, dolomite, strontianite, siderite, calcite, smithonite, witherite, rhodochrosite, otavite, cerrusite. For divalent cations a general expression for an estimation of the reduced partition function (β) from the reduced mass ($\mu = [M_{Cation} \times M_{Carbonate}]/[M_{Cation} + M_{Carbonate}]$) is:

$$1000 \ln \beta = \left(0.032367 - 0.072563 * \frac{10^3}{T} - 0.01073 * \frac{10^6}{T^2}\right) * \mu - 14.003 + 29.953 * \frac{10^3}{T} + 9.4610 * \frac{10^6}{T^2} \quad (2)$$

For Mg-calcite the ^{13}C content varies with the Mg concentration. The fractionation between Mg-calcite (X = mole fraction of $MgCO_3$) and calcite is given by:

$$1000 \ln (\alpha_{Mg_{Calcite} - Calcite}) = \left[0.013702 - 0.10957 \times \frac{10^3}{T} + 1.35940 \times \frac{10^6}{T^2} - 0.329124 \times \frac{10^9}{T^3} + 0.0304160 \times \frac{10^{12}}{T^4}\right] \times X^{1.5} \quad (3)$$

The results of the computations were used together with previously published experimental vaporous CO_2-silicate melt fractionations to determine, at 1200°C, a relationship between melt-CO_2 ^{13}C fractionation and melt composition, expressed as molecular proportions of the cations Mg, Fe, Mn, Ca, Na, K and Si and Al:

$$1000 \ln \alpha_{Melt-CO_2} = 5.14 \times \frac{Mg + Fe + Mn + Ca + Na + K}{Si + Al} + 0.86 \quad (4)$$

A conceptual model to understand this relationship was developed. The results of the computations approximate closely the experimentally determined vaporous CO_2-$CaCO_3$ fractionations at high temperatures. Empirically derived dolomite-calcite and calcite-graphite ^{13}C isotope geothermometers agree with results of the present work. *Copyright © 2004 Elsevier Ltd*

1. INTRODUCTION

The carbon isotope record of volcanic gases provides an important input for the quantification of the Earth's carbon cycle. To interpret the volcanic gas record properly, carbon isotope effects in the degassing of silicate magmas need to be well understood. Available experimental results (Javoy et al., 1978; Mattey et al., 1990; Mattey, 1991; Trull et al., 1992; Blank and Stolper, 1993) indicate that above 1000°C, CO_2 in equilibrium with silicate melts may be enriched in ^{13}C anywhere between 0 and 4‰. The data also indicate that this

* Author to whom correspondence should be addressed (p7d@psu.edu).

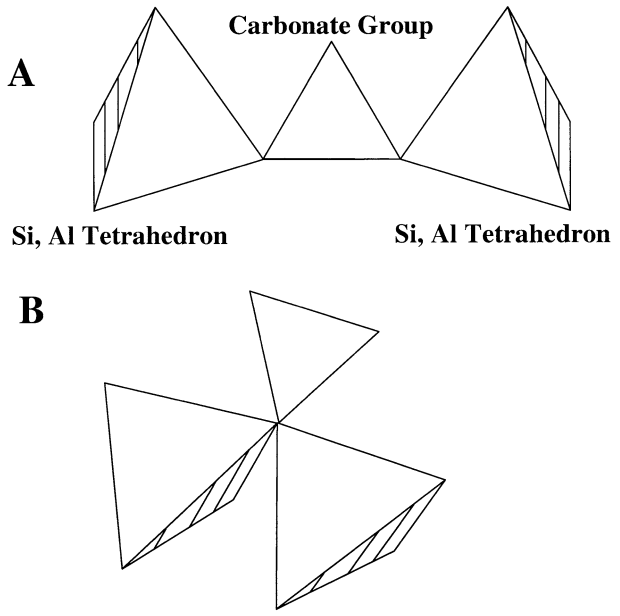

Fig. 1. Bonding of carbonate group in silicate melt structure after Stolper and Fine (1985) (A) and Kohn et al. (1991) (B).

fractionation is, in some way, related to the silicate melt composition; however, how to choose a fractionation factor for a melt of, e.g., a given silica content or other compositional constraints (e.g., the Mg/Fe ratio), remains unclear.

In the review of Blank and Brooker (1994) it is demonstrated that the C solubility depends on melt composition including melt structure, cation and water content, pressure and temperature. The dissolved C is thought to be accommodated in silicate melts mainly in the form of the species CO_2 and CO_3^{2-}. Since the C isotope fractionation properties of the melt species CO_2 and CO_3^{2-} are expected to differ, factors affecting their proportions will cause differences in the melt-vapor C isotope effects.

Molecular CO_2 can occur in the structural voids of melts, similar to the occurrence of noble gases; however, there is NMR evidence that the molecular CO_2 is not free to rotate in a random fashion in the melt structure and that there must be an interaction, albeit weak, between the C atom of the CO_2 molecule and oxygen of the Si/Al tetrahedra. The strength of this interaction varies with melt composition, suggesting a possible C-isotope effect between the gaseous CO_2 and "CO_2" dissolved in silicate melts. Other dissolution mechanisms proposed suggest that the carbonate group can be part of the silicate network of the melt. Two modes have been considered (Fig. 1), in which one or two bridging oxygens may be shared among Si/Al tetrahedra and the carbonate group. In view of the expected differences in force constants of the two forms of C-O bonding, differences in the C isotope fractionation behavior between the two configurations can be expected as well. The formation of Ca and Na carbonate complexes, in the dissolution of CO_2 in silicate melts, has also been proposed. One can expect that carbonate complexes in melts will differ in their C fractionation properties. The observation that water can increase the solubility of CO_2 significantly suggests possible interactions between H_2O and CO_2 in the melt with attendant C isotope effects between C dissolved in the melt and a C-bearing vapor, which would differ from the effects considered so far.

The solubility of C in silicate melts in the presence of methane-dominated fluids was investigated by Taylor and Green (1987). Although the form in which the C occurs in the melt under reducing conditions remains to be established, no spectroscopic evidence for the presence of dissolved CH_4 or other C-H groups has been reported. One can expect, however, that reduced forms of dissolved C would be characterized by distinct isotope effects. If melts are sufficiently reducing, CO may be present in them as well and would show still different C isotope fractionation characteristics.

We can hence conclude that a variety of C-O interactions can occur in silicate melts, and that their nature is melt-composition dependent. One can expect that each of these interactions is associated with a specific isotope effect. The overall isotope fractionation characteristics of a silicate melt will hence depend on: 1. the isotope effects associated with the different C-melt interactions; and 2. the fraction of dissolved C atoms characterized by a particular interaction. The ^{13}C fractionation between a C-containing vapor phase and C dissolved in a silicate melt will be a function of: 1. temperature, 2. pressure, 3. melt composition, and 4. oxygen fugacity. The latter would not only affect the form in which C dissolves in the melt, but also the composition of the fluid, i.e., its $CO_2/CO/CH_4$ ratios.

This paper examines one aspect of the larger problem, i.e., the possible effect of cations in silicate melts on their C isotope fractionation properties. Because the cation-carbonate bonding differs among carbonates and affects their C isotope fractionation characteristics, one can argue that if there is a systematic dependence of the ^{13}C-fractionation on cation-carbonate interactions in carbonates that this dependence ought to carry over, to some extent, into silicate melts. An estimate of the size of the cation effect could hence be obtained by examining the ^{13}C fractionation among carbonates. For this purpose the methodology for computing isotope effects of calcite, developed by Chacko et al. (1991) was used. Since the interest here is to examine the isotope fractionation behavior of one carbonate with respect to another it is imperative that the computation, which includes the selection of the IR frequencies to be used in them, be done consistently for all carbonates considered. In earlier computations (Bottinga, 1968; Chacko et al., 1991) IR frequencies for calcite were selected which produced a best fit to available experimental data for the calcite/CO_2 carbon isotope fractionation. Because such experimental data are not available for other carbonates, this approach to choose frequencies could not be used. In the present study we selected frequencies central to the range of values reported for a particular vibrational mode. For consistency sake the reduced partition function for calcite was therefore re-computed. The results differ from those reported by Chacko et al. (1991). This does not mean that the current results for calcite supercede those of the earlier computations, but rather that they are internally consistent with those obtained for the other carbonates. The important point to note is that we are interested in the difference in fractionation of one carbonate with respect to another. If the results are affected by the manner in which the frequencies were selected, the effect will be similar for all carbonates. Hence, while the absolute values of the reduced partition functions might show an effect, this is less likely to be the case for

the differences among them. Therefore, it was very gratifying to find that the selection process used led, in the case of calcite, to a close match between the computed and experimentally observed fractionations at high temperatures i.e., the temperature range of interest. Because IR data are also available for high pressure $CaCO_3$ polymorphs, the effect of pressure on the C fractionation is examined as well.

2. COMPUTATIONS

To assess the potential effect of cation/carbonate group interactions in melts on the size of the melt/vapor C isotope fractionation, reduced partition functions were computed for polymorphs of $CaCO_3$ and Mg, Fe, Mn, Sr, Ba, Pb, Zn, Cd, Li, and Na carbonates. The computational procedures involve the following steps: 1. choice of the internal and external vibrational frequencies; 2. computation of the frequency shifts which occur when ^{13}C is substituted for ^{12}C in the mineral lattice; 3. evaluation of a Debye temperature, used to approximate the effects of acoustic modes; 4. computation of the reduced partition function. The last step includes the choice of a frequency shift for the modes represented by the Debye term. This frequency shift is selected such that the reduced partition function becomes unity at infinite temperatures.

The results of the computations depend on the vibrational frequencies and their shifts with isotopic substitution, as well as the assumptions made about the contributions of other than the internal vibrational modes to the partition function. Because the results presented here for calcite, deviate from those of earlier computations at low temperatures, the basis of the present work is presented in detail in the Appendix, which includes an analysis of the causes for the differences between the present and earlier results.

While the computations of the reduced partition functions for calcite of Urey and Greiff (1935), Urey (1947), Rubinson and Clayton (1969) and Chacko et al. (1991) treated explicitly only the vibration of the carbonate ion (internal modes), Bottinga (1968) and Golyshev et al. (1981) considered, in addition, vibrations of the carbonate ion with respect to the rest of the calcite lattice explicitly. One might hence expect differences in the results of the two sets of computations. A direct comparison of the published results to assess the effect of an explicit consideration of the lattice vibrations is not very fruitful, however, because both computations considering the external vibrations do not extrapolate to a reduced partition function of unity at infinite temperatures (as theoretically expected). To examine the effect of taking external modes into account explicitly, the vibrational model for the calcite lattice, developed by Giulotto and Loinger (1951), was used (see the Appendix). Force constants, frequencies and frequency shifts were computed, assuming that five external frequencies were known. This approach differs slightly from that taken in the original publication which uses an IR intensity ratio in place of one of the frequencies (note that there is a typographical error in the intensity ratio equation of Giulotto and Loinger, 1951. The correct version can be found in the paper by Loinger, 1950).

A summary of the external modes for calcite used in previous studies and in this work is given in Table A5. A Debye temperature was evaluated by accounting for the contributions of the internal as well as the external modes to the heat capacity and fitting the remainder of the heat capacity with a Debye term. The Debye temperature was evaluated by minimizing the deviation of the experimental data from the computed heat capacity from zero to 298 K. The temperature found for calcite was 261 K.

The reduced partition function of calcite at 300 K is 0.31‰ larger when internal as well as external modes are explicitly considered, than that found when only the internal modes are accounted for explicitly, and all other modes are approximated by a single Debye term.

It is of interest to make a similar comparison for aragonite, the second major structure type of carbonates. However, a detailed analysis of the vibrations within aragonite has not been completed and a force constant model, analogous to that developed for calcite (Giulotto and Loinger, 1951), is not available. The work of Yamamoto et al. (1974) was used to select those external frequencies that could be likened to motions in the Giulotto model, and the frequency shifts computed for calcite were applied. The unit cell of aragonite contains four molecules of $CaCO_3$. The reduced partition function is calculated for a unit cell containing 20 atoms so that there are 60 degrees of freedom. There are four internal modes, two of which are doubly degenerate, leading to six internal modes per carbonate group. The internal frequency shifts were computed according to the model of Heath and Linnett (1948). Because there are four carbonate groups, 24 internal modes are present. This leaves 36 external and acoustic modes. Twenty of these were considered explicitly, which leaves 16 to be represented by the Debye term. In the evaluation of the Debye temperature (430 K) the contribution of the external frequencies to the low temperature heat capacity was considered. Four atoms are exchanged. The reduced partition function for aragonite found on the basis of this very approximate model is, at 300 K, 0.54‰ larger that the reduced partition function obtained when only the internal frequencies are treated explicitly and all other frequencies are represented by a single Debye term.

For both carbonate structures, the difference between reduced partition functions computed considering internal as well as the external modes and those which consider only the internal modes explicitly is small at 300 K. The difference declines with increasing temperature. For this reason, and because the external frequencies have not been properly assigned to all carbonates considered here, the simplified model was used for the computations.

The literature IR spectra for carbonates were reviewed and the frequencies used in the computation of the reduced partition functions for the various carbonates are summarized in Table 1.

3. RESULTS

Computations were carried out from 275 K to 4000 K in steps of 25°C, and tabulated. For efficiency of reporting the results and their usage, the data were then recast into polynomial form using a regression procedure. Various polynomials were fitted to the data and the one predicting the computational results with the smallest variance was chosen. It has the form:

Table 1. Internal frequencies of carbonates used for computations.

Mineral	Composition	Structure	Cation Radius	ν_1 cm^{-1}	ν_2 cm^{-1}	ν_3 cm^{-1}	ν_{3a} cm^{-1}	ν_4 cm^{-1}	ν_{4a} cm^{-1}	Debye Temp K	Data Source for ν[a]
Calcite I	$CaCO_3$	Calcite	1.00	1083	875	1433	1434	713	713	369	1
Calcite II	$CaCO_3$			1096	866	1471	1445	721	715	400	2
Calcite III 20 kbar	$CaCO_3$			1100	868	1537	1513	745	685	400	3
Calcite III 30 kbar	$CaCO_3$			1101.4	867.92	1540	1516.5	746.8	686.7	400	3
Calcite III 40 kbar	$CaCO_3$			1102.8	867.84	1543	1520	748.6	688.4	400	3
Calcite III 50 kbar	$CaCO_3$			1104.2	867.76	1546	1523.5	750.4	690.1	400	3
Calcite III 100 kbar	$CaCO_3$			1111.2	867.36	1561	1541	759.4	698.6	400	3
Aragonite	$CaCO_3$	Aragonite	1.18	1084	862	1472	1481	712	700	383	4
Aragonite 10 kbar	$CaCO_3$	Aragonite	1.18	1086	862	1474	1484	713	702	383	5
Aragonite 20 kbar	$CaCO_3$	Aragonite	1.18	1088	862	1476	1487	715	703	383	5
Aragonite 30 kbar	$CaCO_3$	Aragonite	1.18	1090	862	1479	1490	717	705	383	5
Aragonite 40 kbar	$CaCO_3$	Aragonite	1.18	1092	861	1481	1493	719	706	383	5
Aragonite 50 kbar	$CaCO_3$	Aragonite	1.18	1094	861	1483	1495	721	708	383	5
Aragonite 100 kbar	$CaCO_3$	Aragonite	1.18	1104	859	1494	1510	730	715	383	5
Vaterite	$CaCO_3$	Ca 8 fold	1.12	1083	847	1490	1426	748	748	383	6
Magnesite	$MgCO_3$	Calcite	0.72	1098	885	1465	1465	753	753	530	7
Dolomite	$CaMg(CO_3)_2$	Calcite		1092	881	1441	1441	724	724	453	8
Cerussite	$PbCO_3$	Aragonite	1.35	1053	842	1417	1417	680	680	274	9
Otavite	CdCO3	Calcite	0.74	1090	862	1462	1392	724	728	400	10
Rhodochrosite	$MnCO_3$	Calcite	0.83	1084	866	1426	1426	726	726	405	11
Siderite	$FeCO_3$	Calcite	0.78	1082	868	1447	1445	736	738	372	12
Smithonite	$ZnCO_3$	Calcite	0.74	1093	870	1440	1412	743	733	422	13
Strontianite	$SrCO_3$	Aragonite	1.26	1072	859	1465	1453	704	704	349	14
Witherite	$BaCO_3$	Aragonite	1.47	1062	858	1440	1440	695	695	294	15
	Li_2CO_3	Li 4 fold	0.59	1089	859	1430	1430	740	713	475	16
	Na_2CO_3	Na 4 fold	0.99	1082	883	1425	1413	701	694	292	17

[a] References are as follows:

(1) Mean of data from: Adler et al. (1950), Hunt et al. (1950), Louisfert (1951), Louisfert and Pobeguin (1952), Miller and Wilkens (1952), Huang and Kerr (1960), Weir and Lippincott (1961), Adler and Kerr (1962), Adler and Kerr (1963a, 1963b), Ross and Goldsmith (1964), Chester and Elderfield (1967), Hellwege et al. (1970), Donoghue et al. (1971), Nyquist and Kagel (1971), White (1974), Scheetz and White (1977), Golyshev et al. (1981), Chacko et al. (1991), Böttcher et al. (1993), Jones and Jackson (1993).

(2) From data cited by White (1974).

(3) Mean of data cited by White (1974) and Williams et al. (1992).

(4) Mean of data from: Adler et al. (1950), Hunt et al. (1950), Louisfert (1951), Keller et al. (1952), Louisfert and Pobeguin (1952), Huang and Kerr (1960), Weir and Lippincott (1961), Adler and Kerr (1962), Schroeder et al. (1962), Adler and Kerr (1963a, 1963b), Chester and Elderfield (1967), Rubinson and Clayton (1969), White (1974), French et al. (1980), Golyshev et al. (1981).

(5) Based on the work of Kraft et al. (1991).

(6) Mean of data from: White (1974), Jones and Jackson (1993).

(7) Mean of data from: Hunt et al. (1950), Louisfert (1951), Huang and Kerr (1960), Weir and Lippincott (1961), Adler and Kerr (1963a, 1963b), Ross and Goldsmith (1964), Chester and Elderfield (1967), White (1974), Golyshev et al. (1981), Böttcher et al. (1992) Böttcher et al. (1993).

(8) Mean of data from: Hunt et al. (1950), Louisfert (1951), Huang and Kerr (1960), Weir and Lippincott (1961), Adler and Kerr (1963a, 1963b), Chester and Elderfield (1967), White (1974), Golyshev et al. (1981), Jones and Jackson (1993).

(9) Mean of data from: Louisfert (1951), Huang and Kerr (1960), Schroeder et al. (1962), Adler and Kerr (1963a, 1963b), Ross and Goldsmith (1964), Chester and Elderfield (1967), Golyshev et al. (1981).

(10) White (1974).

(11) Mean of data from: Louisfert (1951), Hunt et al. (1950), Huang and Kerr (1960), Weir and Lippincott (1961), Adler and Kerr (1963a, 1963b), Ross and Goldsmith (1964), Chester and Elderfield (1967), Agiorgitis (1969), White (1974), Golyshev et al. (1981), Böttcher et al. (1992), Böttcher et al. (1993), Jones and Jackson (1993).

(12) Mean of data from: Hunt et al. (1950), Louisfert (1951), Weir and Lippincott (1961), Adler and Kerr (1963a, 1963b), Ross and Goldsmith (1964), White (1974), Golyshev et al. (1981).

(13) Mean of data from: Adler and Kerr (1963a, 1963b), White (1974), Golyshev et al. (1981).

(14) Mean of data from: Adler et al. (1950), Adler and Kerr (1963a, 1963b), Chester and Elderfield (1967), White (1974), Gadsden (1975), Golyshev et al. (1981), Jones and Jackson (1993).

(15) Mean of data from: Louisfert (1951), Huang and Kerr (1960), Schroeder et al. (1962), Adler and Kerr (1963a, 1963b), Ross and Goldsmith (1964), Chester and Elderfield (1967), White (1974), Golyshev et al. (1981).

(16, 17) Data from White (1974). Ionic radii are from Shannon (1976).

$$1000 \times \ln \beta = C_0 + C_1 \frac{10^3}{T} + C_2 \frac{10^6}{T^2} + C_3 \frac{10^9}{T^3} + C_4 \frac{10^{12}}{T^4} \quad (5)$$

The polynomial coefficients are compiled in Table 2. Between the limits of 275 K and 4000 K the relationship reproduces the computed reduced partition function to better than 0.1‰. To achieve this good fit, a constant term had to be included in the polynomial. Regression analyses forcing the relationship to pass through zero at an infinite temperature led to significantly larger deviations of the predicted from the originally computed reduced partition functions. To be sure, however, the reduced

Table 2. Results of computations.

Mineral	Frequency shift fs = ν_i^*/ν_i							Polynomial constants				
	fs_1	fs_2	fs_3	fs_{3a}	fs_4	fs_{4a}	fs_{Debye}	C_0	C_1	C_2	C_3	C_4
Calcite I	1	0.96865	0.97242	0.97242	0.99612	0.99612	0.99724	0.45557	−2.81622	29.9835	−5.02228	0.325816
Calcite II	1	0.97312	0.97312	0.97312	0.97312	0.97312	0.97312	0.46393	−2.87923	30.6567	−5.23505	0.348594
Calcite III 20 kbar	1	0.968646	0.97293	0.97293	0.995597	0.995597	0.997239	0.48197	−3.05729	32.9190	−5.92864	0.420719
Calcite III 30 kbar	1	0.968646	0.972948	0.972948	0.995578	0.995578	0.997239	0.48319	−3.06948	33.0442	−5.96817	0.424965
Calcite III 40 kbar	1	0.968646	0.972967	0.972967	0.995559	0.995559	0.997239	0.48497	−3.07723	33.1435	−5.99919	0.428313
Calcite III 50 kbar	1	0.968646	0.972985	0.972985	0.99554	0.99554	0.997239	0.48816	−3.09845	33.2807	−6.04173	0.432740
Calcite III 100 kbar	1	0.968646	0.973076	0.973076	0.995447	0.995447	0.997239	0.49124	−3.13196	33.8067	−6.20736	0.450491
Aragonite 1 bar	1	0.968646	0.97263	0.97263	0.995904	0.995904	0.997239	0.46953	−2.92915	31.2497	−5.42536	0.368506
Aragonite 10 kbar	1	0.968646	0.972641	0.972641	0.995892	0.995892	0.997239	0.47017	−2.93919	31.3427	−5.45458	0.371666
Aragonite 20 kbar	1	0.968646	0.97266	0.97266	0.995874	0.995874	0.997239	0.46787	−2.93872	31.4208	−5.47890	0.374288
Aagonite 30 kbar	1	0.968646	0.97268	0.97268	0.995853	0.995853	0.997239	0.47274	−2.95991	31.5314	−5.51234	0.377747
Aragonite 40 kbar	1	0.968646	0.972707	0.972707	0.995825	0.995825	0.997239	0.46946	−2.95006	31.5794	−5.52759	0.379278
Aragonite 50 kbar	1	0.968646	0.972725	0.972725	0.995806	0.995806	0.997239	0.47083	−2.95600	31.6430	−5.54614	0.381117
Aragonite 100 kbar	1	0.968646	0.97283	0.97283	0.995699	0.995699	0.997239	0.47420	−2.98767	32.0412	−5.67180	0.394501
Vaterite	1	0.968646	0.973077	0.973077	0.995447	0.995447	0.997239	0.45676	−2.83203	30.2205	−5.15141	0.343185
Magnesite	1	0.968646	0.972691	0.972691	0.995841	0.995841	0.997239	0.46927	−2.92580	31.3429	−5.35141	0.356228
Dolomite	1	0.968646	0.972458	0.972458	0.99608	0.99608	0.997239	0.46250	−2.86130	30.4260	−5.11618	0.333885
Cerussite	1	0.968646	0.972474	0.972474	0.996063	0.996063	0.997239	0.44167	−2.71490	28.8308	−4.77557	0.305748
Otavite	1	0.968646	0.972651	0.972651	0.995882	0.995882	0.997239	0.44213	−2.72040	29.1409	−4.79216	0.304076
Rhodochrocite	1	0.968646	0.972589	0.972589	0.995946	0.995946	0.997239	0.44875	−2.76583	29.5542	−4.90156	0.314405
Siderite	1	0.968646	0.972693	0.972693	0.995839	0.995839	0.997239	0.45599	0.45599	30.2197	−5.10227	0.334594
Smithonite	1	0.968646	0.972713	0.972713	0.995819	0.995819	0.997239	0.45012	−2.77186	29.5765	−4.89827	0.313710
Strontianite	1	0.968646	0.972588	0.972588	0.995947	0.995947	0.997282	0.45870	−2.85960	30.5541	−5.23244	0.349382
Witherite	1	0.968646	0.972479	0.972479	0.996059	0.996059	0.997239	0.45240	−2.80428	29.8711	−5.04177	0.330130
Li_2CO_3	1	0.968646	0.972783	0.972783	0.995747	0.995747	0.997239	0.44853	−2.76570	29.5777	−4.90732	0.315760
Na_2CO_3	1	0.968646	0.972237	0.972237	0.996306	0.996306	0.997239	0.45274	−2.78742	29.5785	−4.90677	0.313380

partition functions computed between 275 K and 4000 K (which served as a basis for the regression polynomials) were carried out such that they smoothly approach zero at infinite temperatures. Extending the computations to 15000 K and fitting a polynomial to the extended data set did not result in a better predictive relationship. In Figure 2 the fractionation between various carbonates and calcite are shown and one observes significant differences among carbonates which vary with temperature.

With increasing temperature the reduced partition functions decline and reach one at infinite temperatures. At a particular temperature, the size of the partition function increases with the vibrational frequencies that are attained within a given carbonate (compare Table 1 and Fig. 2). One can also expect that the reduced partition function increases with the force constants characterizing the carbonate lattice, and that it should decrease with the reduced mass across the cation-carbonate bond.

3.1. Effects of Structure

Calcium carbonate has several polymorphs (Fig. 3) showing significantly different carbon isotope effects (Fig. 4). For aragonite this has been demonstrated previously by Rubinson and

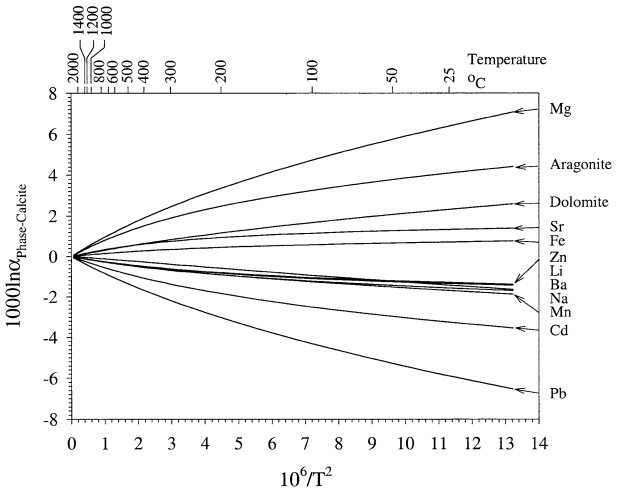

Fig. 2. Carbon isotope fractionation between alkali and alkali earth carbonates and calcite.

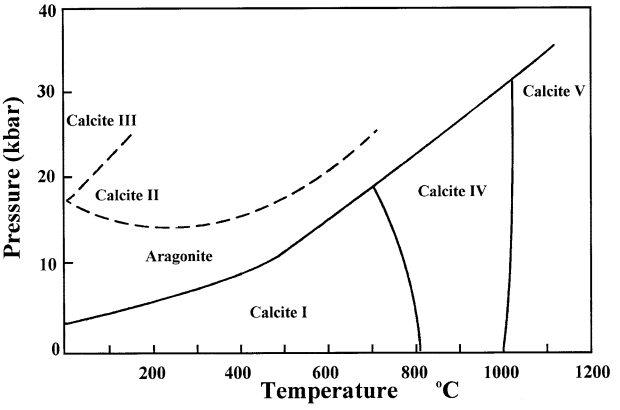

Fig. 3. Phase relationship in the unary system $CaCO_3$ after Carlson (1983). Metastable equilibria are shown as dashed lines.

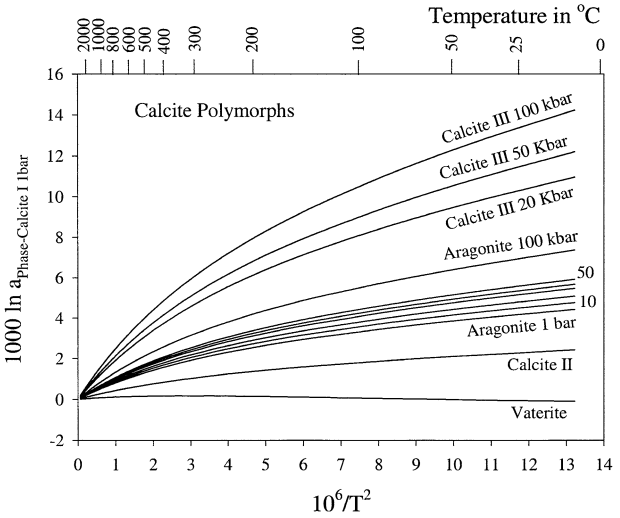

Fig. 4. Carbon isotope fractionation between calcite polymorphs at various pressures compared to calcite I at 1 bar.

Clayton (1969) whose computations indicated a slight (0.9‰) enrichment in ^{13}C in aragonite compared to calcite at 25°C. The computed fractionation is significantly smaller than the 1.8‰ fractionation observed experimentally. The enrichment of 4.12‰ found here is significantly larger than the experimental value. The difference in the computations results from the different choice of vibrational frequencies. The effect of structure on the C isotope fractionation characteristics of $CaCO_3$ (Fig. 4) is elucidated further through computations for the polymorphs, vaterite, calcite II and calcite III, which are metastable with respect to calcite I. It is apparent from Figure 5. that at ambient pressure, the increase in the reduced partition function and hence, the tendency to concentrate the heavy isotope, is directly related to the density of the structure.

Because the carbonate group is fairly rigid and the C-O bond length does not vary significantly between structural types (calcite I, 1.282 Å, Effenberger et al., 1981; calcite II, 1.284 Å;

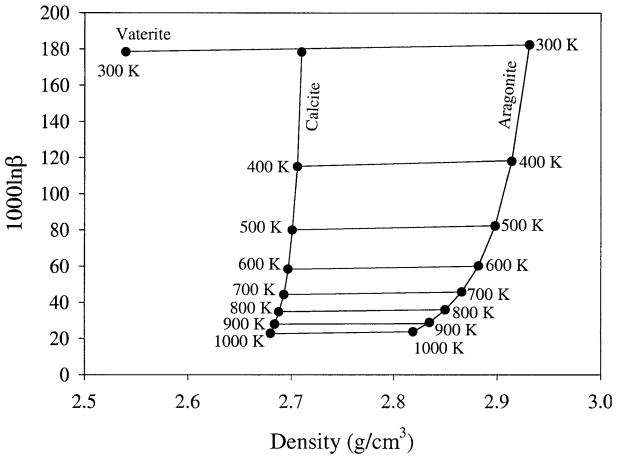

Fig. 5. Relationship between the reduced partition function of $CaCO_3$ polymorphs and their density in the temperature range 300 to 1000 K at 1 bar.

Table 3. Pressure induced internal mode shifts of carbonates, based on the work of Kraft et al. (1991) (1) and Williams et al. (1992) (2).

Phase	Aragonite (1)	Dolomite (1)	Calcite III (2)	Magnesite (2)
Frequency	dν/dP cm^{-1}/GPa	dν/dP cm^{-1}/GPa	dν/dP cm^{-1}/GPa	dν/dP cm^{-1}/GPa
ν1	2.3	3.5	1.4	2.3
ν1	2.0			
ν2	−0.3		−0.08	
ν2	−0.4			
ν3	2.9		3.0	
ν3	2.2		3.5	
ν3			1.5	
ν4	1.4	1.1	1.8	1.5
ν4	1.5		1.7	
ν4	1.8			

aragonite, 1.285 Å; Reeder, 1983), the differences in density among the structures must be the result of differences in the distances between the Ca ions and the carbonate groups. Hence, we may conclude that the carbon isotope fractionation properties vary with the proximity of cations to the carbonate group, and we can expect a similar dependence in silicate melts.

3.2. Effects of Pressure

Based on the observation that there is a direct relationship between in the reduced partition function and the density of the structure, one might expect that the reduced partition function of a particular carbonate mineral would increase with increasing pressure for a given structure type. This is indeed observed. The effect of pressure on the carbon isotope fractionation behavior was investigated by examining the reduced partition function of a particular structure for different pressures. Changes in the IR and Raman spectra with pressure have been observed for aragonite, calcite III, dolomite and magnesite (White, 1974; Kraft et al., 1991; Williams et al., 1992). Table 3 summarizes the observed pressure dependence of internal modes, the only modes considered in the computations reported here (see above). Kraft et al. (1991) note that in the case of aragonite the effect of pressure is larger for the low frequency external modes than for the internal modes. The pressure dependence of the C isotope fractionation was evaluated based on the pressure-dependent IR frequency shifts observed by Kraft et al. (1991) and Williams et al. (1992). Figure 4 demonstrates the effect for aragonite and calcite III for which more detailed data are available (Table 3).

For a given structure the pressure effect $\Delta^{13}C_p = 1000 \ln \beta_{kbar} - 1000 \ln \beta_{kbar\text{-}10}$ (i.e., the change of the reduced partition function/10k bar change in pressure) shows a weak dependence on pressure but varies significantly with temperature. For aragonite, the average pressure effect (‰/10 Kbar) in the pressure range one to 10^5 bars can be expressed as a function of temperature (K) as follows:

$$\Delta^{13}C_{p_{average}} = -0.01796 + 0.06635 * \frac{10^3}{T} + 0.006875 * \frac{10^6}{T^2} \quad (6)$$

Table 4. Effect of pressure on carbon isotope fractionation (‰ per 10 kbar).

T in K	Aragonite	Calcite III	Polyakov and Kharlashina (1994)
500	0.149	0.2075	0.62
750	0.083	0.1163	0.17
1000	0.052	0.0725	0.07
1250	0.035	0.0488	

For calcite III, the pressure effect is found to be on average 1.4 times as large as for aragonite. In view of the similar size of the pressure effect on the frequencies of dolomite and magnesite (Table 3) one can anticipate that these minerals will show similar changes in their reduced partition function with pressure as aragonite and calcite III. The increased pressure leads to a concentration of the heavy isotope in the high pressure polymorph compared to the low pressure form of the mineral. Because lattice frequencies, which show a larger pressure dependence, were not considered explicitly in the computations reported here, the pressure effect on the isotope fractionation could be larger than shown in Figure 4. The computed effects vary from between 0.15 to 0.2‰/10 kbar at 500 K to 0.04 to 0.05‰ at 1250 K and are similar in size to the pressure-dependence for calcite computed by Polyakov and Kharlashina (1994) (Table 4).

Kraft et al. (1991) observed an increased site group splitting of v_3 and v_4 with increasing pressure and suggested that it could arise from either increased asymmetry of the local crystal field surrounding the carbonate ion, or a distortion of the carbonate group. The authors inferred from the observed pressure-enhanced splitting of v_3 that the carbonate group becomes increasingly distorted with increasing pressure. They also suggested that the increase in frequency v_4 results from an increase in the strength of the Ca-O bond and that the change in energy of v_2 in response to pressure reflects changes in the intercarbonate coupling. Williams et al. (1992) interpret the increasing splitting of v_3, the asymmetric stretching mode, in calcite III with increasing pressure also to be the result of an increasing distortion of the carbonate group with increasing pressure. These observations suggest that the pressure effect on the carbon isotope fractionation is a result of distortion of the carbonate group and changes in Ca-O distance, as well as an increase in the intercarbonate coupling. Concerning dolomite, Kraft et al. (1991) note that the frequencies of the two lowest energy vibrations, which result from rotations and translations of the carbonate group with respect to the Mg and Ca cation (see Fig. A2 in Appendix) depend on the largely ionic interaction between the carbonate group and its neighboring divalent cation. The increased energy of these vibrations with pressure indicates that the force constant between neighboring cations and anions increases with increasing pressure. This argues then for a dependence of the C isotope fractionation on the strength of the carbonate-cation interaction. Williams et al. (1992) suggest that it is probable that in magnesite the C-divalent force constant increases more rapidly with pressure than it does within dolomite, hence the former should show a greater dependence of the carbon isotope fraction on pressure than the latter. These considerations lead to the conclusion that silica melt-CO_2 isotope fractionations should also show a pressure dependence and that this pressure dependence may vary with melt composition.

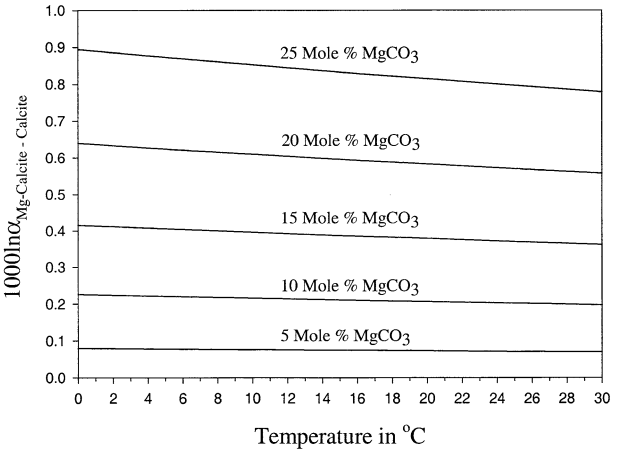

Fig. 6. Dependence of the calcite ^{13}C fractionation on Mg content and temperature at ambient conditions.

3.3. Effects of Composition

The computations for different carbonates, summarized in Figure 2, demonstrate that significant differences in the carbon isotope fractionation exist among them and that these vary with temperature. A systematic increase in the $^{13}C/^{12}C$ ratio from calcite through dolomite to magnesite is suggested by the data. Using the computed reduced partition function for calcite and magnesite, a relationship for the fractionation between Mg-calcite and calcite was sought (using a least squares method) that would accurately predict the computed dolomite-calcite fractionation for a Mg mole fraction of 0.5. The following relationship was determined:

$$1000 \ln(\alpha_{Mg_{Calcite}-Calcite}) = \left[0.013702 - 0.10957 \times \frac{10^3}{T} + 1.35940 \times \frac{10^6}{T^2} - 0.329124 \times \frac{10^9}{T^3} + 0.0304160 \times \frac{10^{12}}{T^4}\right] \times X^{1.5} \quad (7)$$

where X is the mole fraction of $MgCO_3$ in the carbonate. There is extensive solid solution between calcite and dolomite at elevated temperatures (see review of Goldsmith, 1983). One can expect carbon isotopic composition differences between coexisting Mg-calcite and dolomite pairs that will be a function of both temperature and Mg content of the system. High Mg-carbonates are formed at low temperatures as well (see review of McKenzie et al., 1983). Figure 6 demonstrates their carbon isotope fractionation behavior as a function of both temperature and Mg concentration. Sr can show significant concentrations in aragonite. Based on the computations summarized in Figure 2, a significant difference in carbon isotopic composition between pure aragonite and high Sr aragonites can be expected at low temperatures.

Within a given (calcite or aragonite) structure, the reduced partition function tends to decrease with size of the cation (Fig. 7A) and the molar volume of the carbonate (Fig. 7B). Both of

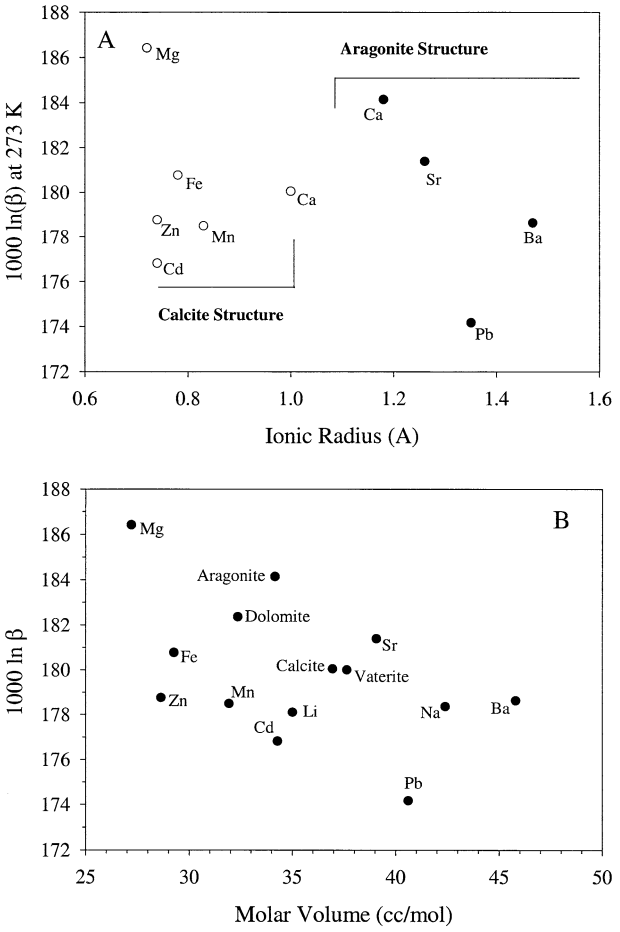

Fig. 7. Dependence of the reduced partition at 298 K and 1 bar on structure, cation radius (A) and molar volume (B).

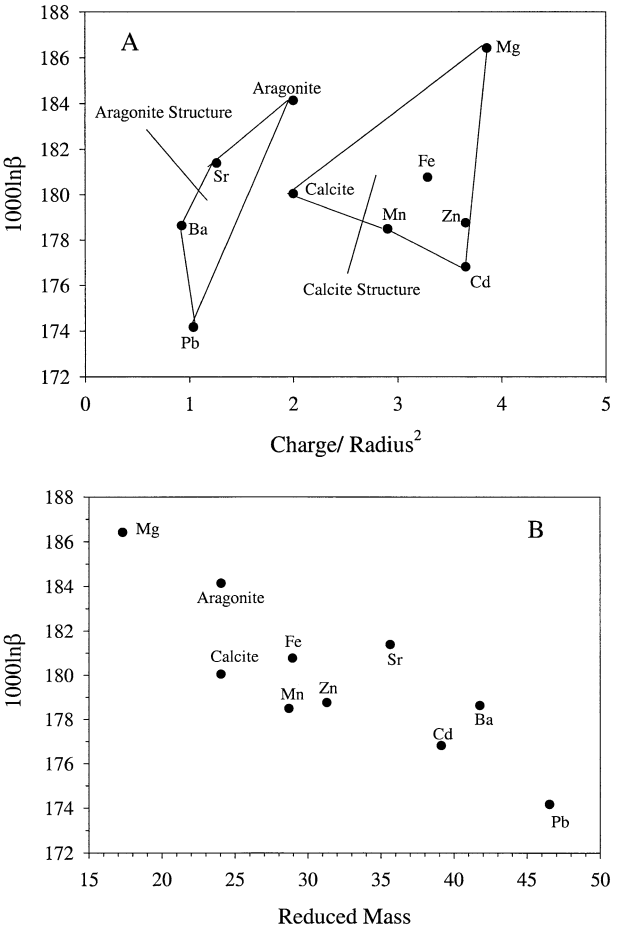

Fig. 8. Dependence of the reduced partition function at 298 K and 1 bar, on the charge/radius (A) ratio and the reduced mass (B).

these trends point to the importance of the nature of the cation on the carbon isotope fractionation property of a carbonate. This notion is confirmed by the positive correlation between the reduced partition function for the carbonates and the charge/radius^2 ratio, which characterizes the electrical field strength of the cation (Fig. 8A).

The reduced mass for the carbonate group-cation interaction provides another measure for the effect of cations on the ^{13}C fractionation properties of carbonates. The energy stored in a bond depends inversely on the square root of the reduced mass. The reduced partition function, and hence the tendency to concentrate the ^{13}C, should increase with decreasing reduced mass characterizing the cation-carbonate bond. This is indeed observed (Fig. 8B) in which the results for divalent carbonates have been presented. The observed trend can be approximated by a linear relationship whose slope and intercept will change with temperature. Regression analyses were carried out on the μ-1000lnβ relationships from 300 to 1400 K at 50 K intervals to determine slopes and intercepts. The resultant set of slopes and intercepts formed smooth relationships with temperature which were fitted to polynomials in 1/T and 1/T^2. The results permit one to write an expression for the reduced partition function as a function of reduced mass and temperature as follows:

$$1000 \ln \beta = \left(0.032367 - 0.072563 * \frac{10^3}{T} - 0.01073 * \frac{10^6}{T^2}\right) * \mu - 14.003 + 29.953 * \frac{10^3}{T} + 9.4610 * \frac{10^6}{T^2} \quad (8)$$

$$\mu = \frac{M_{Cation} * M_{CO_3^{2-}}}{M_{Cation} + M_{CO_3^{2-}}} \quad (9)$$

The value of the reduced partition function predicted by this relationship was compared to the 1000ln β values computed for the carbonates for temperatures from 300 to 1400 K at 50 K intervals (230 comparisons). The relationship predicts the computations based on Table 2 on average to within ±2.4%. The largest deviations observed were +7 and −6%, which occurred at the highest temperatures. The relationship is thus useful for the prediction of the reduced partition function of divalent carbonates. If carbon occurs in silicate melts in the form of carbonate complexes, similar dependencies, and hence effects on the melt-CO_2 carbon isotope fractionation, can be expected.

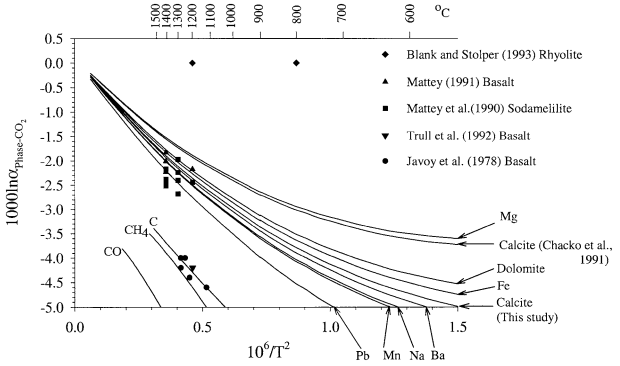

Fig. 9. Comparison of carbon isotope fractionations with respect to CO_2 based on the computed reduced partition function of Chacko et al. (1991) (CO_2, $CaCO_3$), carbonates (this study), Bottinga (1969) (graphite) and Richet et al. (1977) (CH_4, CO), and experimentally measure silica melt-CO_2 fractionations. The results of Chacko et al. (1991), Bottinga (1969) and Richet et al. (1977) were fitted to a polynomial of the form $1000 \ln \beta = C_0 + C_1/T + C_2/T^2 + C_3/T^3 + C_4/T^4$, so that intermediate values could be obtained, and the computations could be extrapolated to higher temperatures.

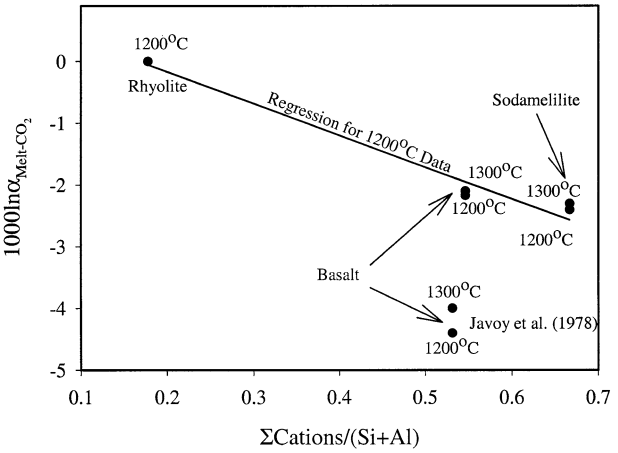

Fig. 10. Dependence of melt-CO_2 carbon isotope fractionation on melt composition. While the 1300°C data have been indicated for comparison, they were not used in the computation of the regression line. The regression is based on the data from Mattey et al. (1990), Mattey (1991) and Blank and Stolper (1993) at 1200°C.

4. DISCUSSION

4.1. Comparison with Experimentally Determined CO_2/Silicate Melt Fractionations

The few available experimentally determined ^{13}C fractionations between silicate melts and vaporous CO_2 are compared in Figure 9 with the computations of Chacko et al. (1991) and this work. The reduced partition function for CO_2 reported by Chacko et al. (1991) was used. Measurements by Mattey et al. (1990) and Mattey (1991) fall close to the fractionations computed here, and are systematically larger than the fractionations computed by Chacko et al. (1991). The results by Blank and Stolper (1993) for rhyolites obviously differ significantly for fractionations expected for carbonate ions or carbonate complexes, and can be understood by appealing to C solution in the melt as molecular CO_2. It should be noted that the pressures at which the experiments were carried out varied from 0.25 to 30 kbar. Assuming that the pressure effect discussed above applies, the pressure correction for the measurements above 1000°C would be below 0.1‰; however, it may be significantly larger for the 800°C determination. The measurements of Javoy et al. (1978) and Trull et al. (1992) are inconsistent with fractionations expected, if C dissolves in silicate melts only as molecular CO_2, carbonate ion or carbonate complexes. The size of the isotopic composition differences observed is close to the fractionation expected between graphite and CO_2. The question whether, under the particular experimental condition used, C dissolved in a reduced form, or whether the experiments are flawed in some way can be answered only through additional experimental studies. In view of this question, we set these measurements aside for the moment.

Based on our computations we have concluded that in carbonate lattices there are interactions between the CO_3^{2-} group and cations such as Mg, Ca, Fe etc. which influence the carbonate/CO_2 carbon isotope fractionation, and that we can expect that such effects will occur in silicate melts as well. On the other hand it has been proposed (Stolper and Fine, 1985; Kohn et al., 1991) that there is an interaction between the Si/Al tetrahedral structure of the melt and the dissolved carbon (Fig. 1). The force constants, and hence the carbon isotope effects governing the cation-carbonate and carbonate-Si/Al tetrahedral structure interaction, will differ significantly and one can expect that there should be a relationship between the relative importance of these two chemical variables and the melt/CO_2 carbon isotope fractionation. The molar ratio of the sum of the cations of Mg, Fe, Mn, Ca, Na, K, characterizing the cation interaction, to the sum of Si + Al, characterizing the interaction with the silicate melt, is a measure of the relative importance of the two interactions. Figure 10 shows this relationship. Because the fractionations measured by Javoy et al. (1978) and Trull (1992) cannot be understood on the basis of oxidized carbon species but require the presence of a reduced form of C, they were not considered in the computation of the regression for 1200°C, which is represented by:

$$1000 \ln \alpha_{\text{Melt}-CO_2} = 5.14 \times \frac{\text{Mg} + \text{Fe} + \text{Mn} + \text{Ca} + \text{Na} + \text{K}}{\text{Si} + \text{Al}} + 0.86 \quad (10)$$

This relationship is interpreted as reflecting the overall effect of the presence of cations. It is to be noted, however, that Figure 2 also indicates that the nature of the cation can be expected to affect the size of the fractionation, which could vary, depending on the relative abundances of Mg, Fe, Mn, Ca and Na by as much as 0.8‰ at 1000°C. More careful experimental determinations of the melt-CO_2 fractionation as a function of melt composition are necessary to isolate the size of the isotope effects of various C dissolution mechanisms. The available very scanty data provide, however, an indication of the nature of the dependence of melt-CO_2 isotope fractionations on melt composition.

The complexity of the dependence of the carbon isotope fractionation between a vapor and a melt can be best explained by writing a general expression for this fractionation:

$$\alpha_{v-m} = \frac{\sum_{i=1}^{n_v} x_i^v \times \alpha_{i-r}^v}{\sum_{j=1}^{n_m} x_j^m \times \alpha_{j-r}^m} \quad (11)$$

where

α_{v-m} = fractionation factor between vapor and melt,

α_{i-r}^v = fractionation factor between vapor species i and a reference species (e.g., gaseous CO_2),

α_{j-r}^m = fractionation factor between melt species j and the reference species (e.g., gaseous CO_2),

x_i^v = mole fraction of C present in vapor as species i,

x_j^m = mole fraction of C present in melt as species j,

n_v = number of C species in vapor,

n_m = number of C species in melt.

The vapor-melt fractionation, for a vapor, containing potentially carbon dioxide, methane and carbon monoxide, and a melt, containing potentially dissolved carbon dioxide, C interacting with the silicate melt structure, carbonate complexes of various types, as well as C dissolved in some reduced form (s), can be written as:

$$\alpha_{v-m} = \frac{1 \times x_{CO_2} + \alpha_{CH_4} \times x_{CH_4} + \alpha_{CO} \times x_{CO}}{\alpha_{mCO_2} \times x_{mCO_2} + \alpha_{Si-St} \times x_{Si-St} + \sum_{jCO_3-Complexes} \alpha_{jCO_3} \times x_{jCO_3} + \sum_{jReduced} \alpha_{jRed} \times x_{jRed}} \quad (12)$$

where

mCO_2 = CO_2 dissolved in melt in molecular form,

Si-St = C interacting with silicate structure,

jCO_3-Complexes = Mg, Ca, Fe, Na etc. carbonate complexes,

jReduced = carbon in reduced chemical forms, e.g., CO

All fractionation factors, α, are expressed with respect to gaseous CO_2. The fractionation factor $\alpha_{Melt\text{-}CO2}$ discussed above represents the integrated effect of α_{mCO2}, $\alpha_{Si\text{-}St}$, and α_{jCO3}. The mole fractions, x^v_i, in the vapor are affected by pressure and temperature and oxygen fugacity. The effect of these three variables on the vapor composition and its isotope fractionation behavior have been explored in some detail by Deines (1980). The temperature dependence of the reduced partition functions of CO_2, CH_4 and CO have been well established through theoretical computations (e.g., Richet et al., 1977); their pressure dependence has not been explored in detail. Considering the C species in the melt, one can expect a pressure-, temperature—as well as composition—dependence of the mole fractions x^m_j. The oxygen fugacity will have significant effects on the x_{jRed} term (s).

Although progress has been made in the understanding of the C speciation in silicate melts, a quantification of the various x^m_j terms is not possible at this time. Likewise one cannot quantify all of the necessary isotope fractionation properties of the various melt species to be able to evaluate $\alpha_{v\text{-}m}$. However, even the exceedingly limited experimental data, in combination with the present computation, can provide some insight into the compositional dependence of the vapor melt fractionation.

At 1200°C the vapor/melt fractionation has been determined for three significantly different melt compositions. As these experiments were carried out under sufficiently oxidizing conditions, the reduced species can be neglected in the vapor/melt fraction expression above. The relationship can be further simplified by noting that at 1200°C the fractionation properties of the Ca, Fe and Na carbonates are reasonably similar and can be approximated by a single fractionation (α_{CatCO3}). This is not true for magnesium. With these simplifying assumptions the vapor/melt fractionation becomes:

$$\alpha_{v-m} = \frac{x_{CO_2}}{\alpha_{mCO_2} \times x_{mCO_2} + \alpha_{Si-St} \times x_{Si-St} + \alpha_{CatCO_3} \times x_{CatCO_3} + \alpha_{MgCO_3} \times x_{MgCO_3}} \quad (13)$$

The mole fractions $X_{Si\text{-}St}$, X_{CatCO3}, X_{MgCO3} can be estimated from the melt composition. The fractionation factors α_{mCO2}, α_{CatCO3}, α_{MgCO3} can be characterized by the computed reduced partition functions but $\alpha_{Si\text{-}St}$ and X_{CO2} are unknown. In view of the size of the fractionations observed for the sodamellite and basalt melt compared to the rhyolite melt, and the observation that the fraction of C dissolved as CO_2 declines from rhyolitic to basaltic melt compositions, it was assumed that for the former two, X_{CO2} was small (less than 10%) compared to $X_{Si\text{-}St} + X_{CatCO3} + X_{MgCO3}$. With these simplifications and assumptions one can find an estimate for the reduced partition function for the C interacting with the Si/Al tetrahedra of the melt. The vapor-melt fractionations measured for sodamellite and basalt melts, both yield an estimate of ~11 for 1000 ln β, which varies by a bout 0.2 when X_{CO2} is varied from zero to 10%.

The rhyolite melt-vapor fractionation appears to be dominated by the fractionation characteristics of CO_2. A melt-vapor fractionation of exactly zero‰, as reported, could imply that: *a.* vaporous and dissolved CO_2 behave identically and that dissolved C does not interact with the melt or *b.* the model above applies, but that there is a compensation of isotope effects, i.e., the CO_2 in the melt does not behave isotopically identically to the vaporous CO_2. While proposition *a* is less satisfactory than proposition *b*, one needs to consider also the most likely possibility that the vapor-melt fractionation is actually not identical to zero. One can use the estimated reduced partition function for the C-Si/Al tetrahedra interaction, and Eqn. 13 to examine the relationship between the rhyolite melt-vapor fractionation and the fraction of C present as dissolved CO_2. One finds that if the melt-vapor fraction were −0.2‰, in stead of zero, 10%

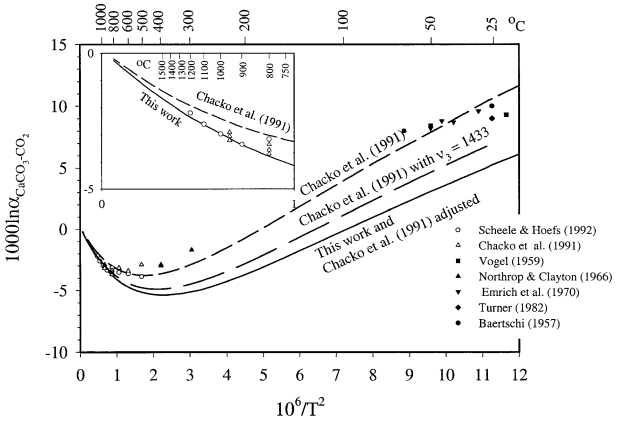

Fig. 11. Experimentally determined and computed carbon isotope fractionation between calcite and CO_2.

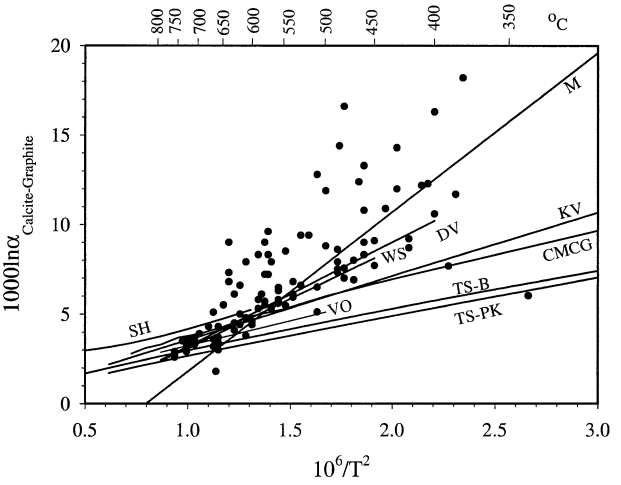

Fig. 12. ^{13}C fractionation between calcite and graphite. Comparison of empirical fractionations: VO = Valley and O'Neil (1981), WS = Wada and Suzuki (1983), M = Morikiyo (1984), DV = Dunn and Valley (1992), KV = Kitchen and Valley (1995); experimental determinations: SH = Scheele and Hoefs (1992); previous computations: CMCG = Chacko et al. (1991); this study: TS-B = this study's calcite reduced partition function combined with the graphite partition function for graphite of Bottinga (1969), TS-PK = this study's calcite reduced partition function combined with the graphite partition function for graphite of Polyakov and Kharlashina (1995); and fractionations observed in metamorphic rocks (solid circles): data from Valley and O'Neil (1981), Wada and Suzuki (1983), Kreulen and Beek (1983) Morikiyo (1984), Kitchen and Valley (1995), Rathmell et al. (1999). The temperature estimates for the metamorphic rocks were taken from the original publications and were based on element distributions and mineral stability data.

of C in the melt could be interacting with the silicate structure and or be present in the form of carbonate complexes.

Although the data permit some insights, they are obviously too limited to come to firm conclusions. The analysis of the dependence of $\alpha_{v\text{-}m}$ on physical and chemical parameters is fruitful, however, because it demonstrates what the variables are that need to be controlled, or measured in laboratory experiments aimed at a complete understanding of the carbon isotope fractionation properties of silicate melts.

4.2. Comparison with CO_2/Calcite Fractionations

A larger number of experimental determinations, over a wider temperature range, are available for the $CaCO_3$-$CO_{2(vapor)}$ fractionation. They are compared with the theoretical computations in Figure 11. The results of the present computations provide a better fit to the data above 700°C than the computations of Chacko et al. (1991) which are seen to provide a better fit for the low temperature measurements, a result of the particular choice of frequencies and frequency-shift factors made by the authors (see the Appendix). The result of simply changing the wave number for ν_3 in the computation of these authors to a more commonly observed value, is shown in the figure as well. The rather large effect on the computed fractionation is apparent. If all of the parameters are adjusted as discussed in the Appendix, the computations of Chacko et al. (1991) and the present computations coincide, and the good fit at low temperatures disappears. The good fit of the high temperature experiments for $CaCO_3$ with the high temperature computations of this study gives us confidence that at *high temperatures* the results of this work represent closely the C-isotope fractionation properties of carbonates. The mismatch at lower temperatures is likely to be related to the incompleteness of the vibrational model used for the computations, a limitation that was recognized earlier by Urey (1947) and Rubinson and Clayton (1969) and is not significantly improved upon by considering lattice modes vibrations using the model of Giulotto and Loinger (1951).

4.3. Calcite-Graphite ^{13}C Fractionation

The carbon isotope fractionation between calcite and graphite is of considerable interest as it has the potential to provide temperature information about metamorphic processes. Valley and coworkers have attempted to calibrate this isotope thermometer empirically, using mineral stability and composition data. Theoretical computations by Bottinga (1968, 1969), Chacko et al. (1991) and Polyakov and Kharlashina (1995) have provided a second method of calibration and Scheele and Hoefs (1992) have measured the fractionation as a function of temperature experimentally. The available information has been compiled in Figure 12. Also shown are two calibration curves based on the calcite-reduced-partition function computed in this study and the computations for graphite of Bottinga (1969) and Polyakov and Kharlashina (1995). The latter authors combined their computations for graphite with those of Chacko et al. (1991) for calcite to find a $\Delta^{13}C_{calcite\text{-}graphite}$ temperature calibration. The resulting relationship coincides with the empirical calibration of Valley and O'Neil (1981). Polyakov and Kharlashina (1995) therefore suggested that this coincidence indicates that their computations reflect more properly the ^{13}C fractionation properties of graphite than the results of Bottinga (1969). Aside from the well-known difficulty to use observed isotope fractionations between mineral pairs to argue for or against the validity of isotope thermometers, the dependence of the results of Chacko et al. (1991) on the chosen IR frequency discussed above should be noted. Valley and coworkers have pointed out the fact that the calibration of Chacko et al. (1991) yields too large fractionations at a particular temperature and this has been also discussed by Chacko et al. (1991). The comparison of the computations of the present

Table 5. Sensitivity of calcite-graphite ^{13}C isotope thermometer.

	Slope	
	2.4	2.8
t °C	‰/100°C	‰/100°C
500	1.04	1.21
600	0.72	0.84
700	0.52	0.61
800	0.39	0.45
900	0.30	0.35
1000	0.23	0.27

work with experimental data for the $CaCO_3$-CO_2 fractionation (Fig. 12) leads to the same conclusion, i.e., that the reduced partition function for calcite reported by Chacko et al. (1991) is too large. Hence the fit of the Polyakov and Kharlashina's (1995) calibration with the empirical calibration of Valley and O'Neil (1981) may be fortuitous. The combination of the calcite reduced partition of this study with the results of Bottinga (1969) yields fractionations falling closer to the empirical calibration of Valley and O'Neil (1981), while the combination with the work of Polyakov and Kharlashina (1995) yields smaller fractionations. While the question of which of the results for the graphite-reduced-partition function are more reliable remains to be settled, it is interesting to note, in Figure 12, that the slopes of the "calibrations" VO (slope = 2.8), TS-B (slope = 2.5) and TS-PK (slope = 2.4) as well as SH (slope = 2.4) are very similar in the temperature range shown. Hence, temperature *sensitivity* of the thermometer has been reasonably well established (Table 5).

4.4. The Dolomite-Calcite Carbon Isotope Fractionation

Schwarcz (1966) pointed out the potential use of the ^{13}C fractionation between dolomite and calcite as a geothermometer, and the possibility of calibrating it empirically through temperature estimates based the Mg content of magnesian calcite and the solvus in the system calcite-dolomite (Goldsmith and Graf, 1958; Graf and Goldsmith, 1958; Goldsmith and Heard, 1961; Goldsmith and Newton, 1969; Anovitz and Essene, 1987). In Figure 13 measured $\Delta^{13}C_{dolomite\text{-}calcite}$ and estimated temperatures, mainly from solvus data, are shown along with the empirical calibrations of Wada and Suzuki (1983) and Sheppard and Schwarcz (1970). Sheppard and Schwarcz (1970) also reported the results of an experimental determination of this fractionation as a function of temperature, which deviates rather significantly from the empirical calibrations. While some of the naturally observed data follow the experimental fractionation line, most data scatter around the calibration curve of Sheppard and Schwarcz (1970). Rathmell et al. (1999) have pointed out that the calcite-dolomite thermometer is sensitive to resetting during deformation and retrogression, and therefore the use of solvus temperature estimates may not be the best tool to establish a calibration for the $\Delta^{13}C_{Dolomite\text{-}Calcite}$ thermometer. It is therefore gratifying to note the close agreement between the results of the present computations and the empirical calibration of Sheppard and Schwarcz (1970), lending support for the validity of the sample selection criteria used by these authors in their calibration.

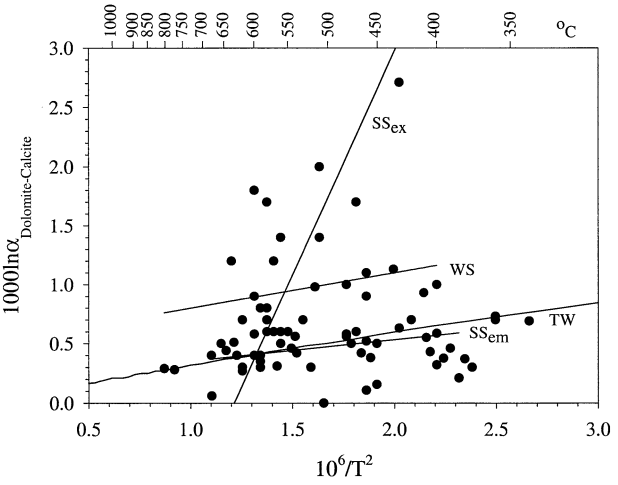

Fig. 13. Carbon isotope fractionation between coexisting dolomite-calcite pairs as a function of temperature of metamorphic hydrothermal, and carbonatite carbonates. Data are from Jia and Kerrich (2000), Richards et al. (1996), Knudsen and Buchardt (1991), Wada and Suzuki (1983), Wada and Oana (1975), Sheppard and Schwarcz (1970), and Schwarcz (1966). The temperature information was derived mainly from the solvus temperature of magnesian calcite. The empirical calibrations of Wada and Suzuki (1983) (WS) and Sheppard and Schwarcz (1970) (SS_{em}), the experimental determination of Sheppard and Schwarcz (1970) (SS_{ex}), and the fractionation computed in this work (TW) are also shown.

5. CONCLUSIONS

The results of the computations of the reduced partition function for carbonates suggest that the carbon isotope fractionation properties of silicate melts will depend on the melt structure, its density, the proximity of the cations to the carbonate group, distortion of the carbonate group, the strength of the cation-carbonate group interaction, as well as any intercarbonate coupling. They also suggest that the fractionation should be pressure dependent and that the size of this pressure dependence could vary with melt composition.

The nature of the cations present in the melt can be expected to have an effect on the carbon isotope fractionation property of a silicate melt. In particular one can anticipate differences in the fractionation that depend on the size of the melt's Mg/Fe, Mg/Ca and Mg/Na ratios. A second important chemical parameter influencing the melt/vapor carbon isotope fractionation is the melt's cation/(Si + Al) ratio. The^{13}C fractionation between melt and CO_2 increases systematically with increasing ΣCation/(Si + Al) ratio. Overall, the silicate melt-vapor ^{13}C fractionation will be a function of P, T, silicate melt composition and oxygen fugacity.

The dependence of the C isotope fractionation properties of silicate melts on these chemical parameters is complicated and can be elucidated only through carefully conducted experimental studies. The fractionation model that has been developed in this paper can be used to demonstrate how the effects of individual variables could be isolated in such experiments.

The results for the individual carbonates demonstrate that

their C isotope fractionation is related to the nature of the cation, its size, charge density and reduced mass. The computed pressure effects on the reduced partition function of carbonates vary from between 0.15 to 0.2‰/10kbar at 500 K to 0.04 to 0.05‰ at 1250 K and are similar in size to the pressure dependence for calcite computed by Polyakov and Kharlashina (1994). The ^{13}C fractionation of carbonates, showing the phenomenon of solid solution, varies systematically with the solid solution composition. At all temperatures the ^{13}C fractionation between Mg-calcite and pure $CaCO_3$ increases with increasing Mg content and a quantitative relationship for the dependence was derived. Sr can show significant concentrations in aragonite. Based on the present computations significant difference in carbon isotopic composition between pure aragonite and high Sr aragonites can be expected at low temperatures.

The $CaCO_3$-CO_2 ^{13}C fractionation deduced from the present computations matches closely experimental data at high temperatures, but not at low temperatures. This is in contrast to earlier computations that fit the experimental data better at low temperatures than at high temperatures. The difference in results is traced to the choice of vibrational frequencies and frequency shifts used in the earlier computations.

The fractionation between calcite and graphite deduced by combining the calcite reduced partition function of this study with the results of Bottinga (1969) for graphite yields fractionations falling close to the empirical calibration of Valley and O'Neil (1981), however the combination with the computations for graphite of Polyakov and Kharlashina (1995) yields smaller fractionations. While the absolute ^{13}C fractionation between calcite and graphite needs to be determined with greater accuracy, the temperature *sensitivity* of the thermometer has been reasonably well established.

There is good agreement between the dolomite-calcite ^{13}C fractionation computed in this study with the empirical temperature calibration of the thermometer by Sheppard and Schwarcz (1970).

Acknowledgments—The paper benefitted greatly from discussions with W. B. White, and the author gratefully acknowledges his contribution. Financial support was in part provided through NSF Grant EAR96-27324 to P. Deines.

Associate editor: S. M. F. Sheppard

REFERENCES

Adler H. H., Bray E. E., Stevens N. P., Hunt J. M., Keller W. D., Pickett E. E., and Kerr P. F. (1950) Infrared spectra of reference clay minerals. Preliminary Report 8. *Am. Petrol. Inst. Proj.* **49,** 7–71.

Adler H. H. and Kerr P. F. (1962) Infrared study of aragonite and calcite. *Am. Mineral.* **47,** 700–717.

Adler H. H. and Kerr P. F. (1963a) Infrared absorption frequency trends for anhydrous normal carbonates. *Am. Mineral.* **48,** 124–137.

Adler H. H. and Kerr P. F. (1963b) Infrared spectra of some carbonate minerals. *Am. Mineral.* **48,** 839–853.

Agiorgitis G. (1969) Über differential-thermoanalytische und infrarotspektroskopische Untersuchungen von Mangan-Mineralien. *Tschermaks Miner. Petrogr. Mitt.* **13,** 273–283.

Anovitz L. M. and Essene E. J. (1987) Phase equilibria in the system $CaCO_3$-$MgCO_3$-$FeCO_3$. *J. Petrol.* **28,** 389–414.

Baertschi P. (1957) Messung and Deutung relativer Häufigkeitsvariationen von O^{18} und C^{13} in Karbonatgesteinen und Mineralien. *Schweizerische Miner. Petrogr. Mitt.* **37,** 73–152.

Becker R. H. (1971) Carbon and oxygen isotope ratios in iron formation and associated rocks from the Hamersley Range of Western Australia and their implications. Ph.D. dissertation. University of Chicago.

Blank J. G. and Stolper E. M. (1993) The partitioning of ^{13}C between coexisting CO_2 vapor and rhyolitic melt. *Eos* **74,** 347–348.

Blank J. G. and Brooker R. A. (1994) Experimental studies of carbon dioxide in silicate melts: Solubility, speciation and stable carbon isotope behavior. In *Volatiles in Magmas*, pp. 157–186. Reviews in Mineralogy 30.

Böttcher M. E., Gehlken P.-L., and Usdowski E. (1992) Infrared spectroscopic investigations of the calcite-rhodochrocite and parts of the calcite-magnesite mineral series. *Contrib. Mineral. Petrol.* **109,** 304–306.

Böttcher M. E., Gehlken P.-L., Usdowski E., and Reppke V. (1993) An infrared spectroscopic study of natural and synthetic carbonates from the quaternary system $CaCO_3$-$MgCO_3$-$FeCO_3$-$MnCO_3$. *Z. Dt. Geol. Ges.* **144,** 478–484.

Bottinga Y. (1968) Calculation of fractionation factors for carbon and oxygen isotopic exchange in the system calcite-carbon dioxide-water. *J. Phys. Chem.* **72,** 800–807.

Bottinga Y. (1969) Calculated fractionation factors for carbon and hydrogen isotope exchange in the system calcite-carbon dioxide-graphite-methane-hydrogen-water vapor. *Geochim. Cosmochim. Acta* **33,** 49–64.

Carlson W. D. (1983) The polymorphs of $CaCO_3$ and the aragonite-calcite transformation. In *Carbonates: Mineralogy and Chemistry*, pp. 191–225. Reviews in Mineralogy 11.

Chacko T., Mayeda T. K., Clayton R. N., and Goldsmith J. R. (1991) Oxygen and carbon isotope fractionation between CO_2 and calcite. *Geochim. Cosmochim. Acta* **55,** 2867–2882.

Chester R. and Elderfield H. (1967) The application of infra-red absorption spectroscopy to carbonate minerals. *Sedimentology* **9,** 5–21.

Deines P. (1980) The carbon isotopic composition of diamonds: relationship to diamond shape, color, occurrence and vapor composition. *Geochim. Cosmochim. Acta* **44,** 943–961.

Donoghue M., Hepburn P. H., and Ross S. D. (1971) Factors affecting the infrared spectra of planar anions with D_{3h} symmetry-V. The origin of the splitting of the out-of-plane bending mode in carbonates and nitrates. *Spectrochim. Acta* **27A,** 1065–1072.

Dunn S. R. and Valley J. W. (1992) Calcite-graphite isotope thermometry: A test for polymetamorphsim in marble, Tudor gabbro aureole, Ontario, Canada. *J. Metamorphic Geol.* **10,** 487–501.

Effenberger H., Mereiter K., and Zemann J. (1981) Crystal structure refinement of magnesite, calcite, rhodochrocite, siderite. smithonite, and dolomite, with discussion of some aspects of the streochemistry of calcite type carbonates. *Z. Kristallogr.* **156,** 233–234.

Emrich K., Ehalt D. H., and Vogel J. C. (1970) Carbon isotope fractionation during the precipitation of calcium carbonate. *Earth Planet. Sci. Lett.* **8,** 363–371.

French R., Wang E. C., and Bates J. B. (1980) The i. r. and Raman spectra of $CaCO_3$ (aragonite). *Spectrochim. Acta* **36A,** 915–919.

Gadsden J. A. (1975) *Infrared Spectra of Minerals and Related Inorganic Compounds*. Butterworths.

Giulotto L. and Loinger A. (1951) Oscillazioni esterne e calore specifico della calcite. *Nuovo Cimento* **8,** 475–486.

Goldsmith J. R. (1983) Phase relations of rhombohedral carbonates. In *Carbonates: Mineralogy and Chemistry* (ed. R. J. Reeder), pp. 49–76. Reviews in Mineralogy 11.

Goldsmith J. R. and Graf D. L. (1958) Relation between the lattice constants and the composition of Ca-Mg carbonates. *Am. Mineral.* **43,** 84–101.

Goldsmith J. R. and Heard H. C. (1961) Subsolidus phase relations in the system $CaCO_3$-$MgCO_3$. *J. Geol.* **69,** 45–74.

Goldsmith J. R. and Newton R. C. (1969) P-T-X relations in the system $CaCO_3$-$MgCO_3$ at high temperatures and pressures. *A. J. Sci.* **267A,** 160–190.

Graf D. L. and Goldsmith J. R. (1958) The solid solubility of $MgCO_3$, in $CaCO_3$: A revision. *Geochim. Cosmochim. Acta* **13,** 218–219.

Golyshev S. I., Padalko N. L., and Pechenkin S. A. (1981) Fractionation of stable oxygen and carbon isotopes in carbonate systems. *Geochem. Intern.* **18,** 85–99.

Heath D. F. and Linnett J. W. (1948) Molecular force fields. Part III. The vibration frequencies of some planar XY_3 molecules. *Trans. Faraday Soc.* **44,** 873–878.

Hellwege K. H., Lesh W., Plihal M., and Schaack G. (1970) Zwei-Phononen-Absorptionsspektren und Dispersion der Schwingungszweige in Kristallen der Kalkspatstructur. *Z. Physik* **232,** 61–86.

Herzberg G. (1945) *Infrared and Raman Spectra of Polyatomic Molecules*. D. Van Nostrand.

Hexter R. M. (1958) High resolution, temperature dependent spectra of calcite. *Spectrochim. Acta* **10,** 81–290.

Huang C. K. and Kerr P. F. (1960) Infrared study of the carbonate minerals. *Am. Mineral.* **45,** 311–324.

Hunt J. M., Wisherd M. P., and Bonham L. C. (1950) Infrared absorption spectra of minerals and other inorganic compounds. *Anal. Chem.* **22,** 1478–1497.

Javoy M., Pineau F., and Iiyama I. (1978) Experimental determination of the isotopic fractionation between gaseous CO_2 and carbon dissolved in tholeiitic magma: A preliminary study. *Contrib. Mineral. Petrol.* **67,** 35–39.

Jia Y. and Kerrich R. (2000) Giant quartz vein systems in accretionary orogenic belts: The evidence for a metamorphic fluid origin from delta $\delta^{15}N$ and $\delta^{13}C$ studies. *Earth Planet Sci. Lett.* **184,** 211–224.

Jones G. C., Jackson B. (1993) *Infrared Transmission Spectra of Carbonate Minerals*. Chapman and Hall.

Keller W. D., Spotts J. H., and Biggs D. L. (1952) Infrared sectra of some rock-forming minerals. *Am. J. Sci.* **250,** 453–471.

Kitchen N. E. and Valley J. W. (1995) Carbon isotope thermometry in marbles of the Adirondack Mountains, New York. *J. Metamorphic Geol.* **13,** 577–594.

Knudsen C. and Buchardt B. (1991) Carbon and oxygen isotope composition of carbonates from the Qaqarssuk carbonatite complex, southern West Greenland. *Chem. Geol. Isotope Geosci. Sect.* **86,** 263–274.

Kohn S. C., Brooker R. A., and Dupree R. (1991) ^{13}C MAS NMR: A method for studying CO_2 speciation in glasses. *Geochim. Cosmochim. Acta* **55,** 3879–3884.

Kraft S., Knittle E., and Williams Q. (1991) Carbonate stability in the earth mantle: A vibrational spectroscopic study of aragonite and dolomite at high pressures and temperatures. *J. Geophys. Res* **96 (***B11***),** 17997–18009.

Kreulen R. and van Beek P. C. J. M. (1983) The calcite-graphite isotope thermometer: Data on graphite bearing marbles from Naxos, Greece. *Geochim. Cosmochim. Acta* **47,** 1527–1530.

Loinger A. (1950) Sull'intensità delle righe esterne Raman e infrarosse dei cristalli. *Nuovo Cimento* **7,** 939–942.

Louisfert J. (1951) Spectres d'absorption infrarouges de carbonates métalliques á l'état de poudre. *Compt. Rend. Hebd. Acad. Sci. Paris* **233,** 381–385.

Louisfert J. and Pobeguin T. (1952) Différenciation, au moyen des spectres d'absorption infrarouges, des carbonates de calcium. *Compt. Rend. Hebd. Acad. Sci. Paris* **235,** 287–289.

Mattey D. P. (1991) Carbon dioxide solubility and carbon isotope fractionation in basaltic melt. *Geochim. Cosmochim. Acta* **55,** 3467–3473.

Mattey D. P., Taylor W. R., Green D. H., and Pillinger C. T. (1990) Carbon isotopic fractionation between CO_2 vapour, silicate and carbonate melts: An experimental study at 30 kbar. *Contrib. Mineral. Petrol.* **104,** 492–505.

McCrea J. M. (1950) On the isotopic chemistry of carbonates and a paleotemperature scale. *J. Chem. Phys.* **18,** 849–857.

McKenzie F. T., Bischoff W. D., Bishop F. C., Loijens M., Schoonmaker J., Wollast R. (1983) Magnesian calcites: Low-temperature occurrence, solubility and solid-solution behavior. In *Carbonates: Mineralogy and Chemistry* (ed. R. J. Reed), pp. 97–144. Reviews in Mineralogy 11.

Miller F. A. and Wilkens C. H. (1952) Infrared spectra and characteristic frequencies of inorganic ions. *Anal. Chem.* **24,** 1253–1294.

Morikiyo T. (1984) Carbon isotopic study on coexisting calcite and graphite in the Ryoke metamorphic rocks, northern Kiso District, central Japan. *Contrib. Mineral. Petrol.* **87,** 251–259.

Northrop D. A. and Clayton R. N. (1966) Oxygen-isotope fractionations in systems containing dolomite. *J. Geol.* **74,** 174–196.

Nyquist R. A. and Kagel R. O. (1971) *Infrared Spectra of Inorganic Compounds.* Academic Press.

Polyakov V. B. and Kharlashina N. N. (1994) Effect of pressure on equilibrium isotopic fractionation. *Geochim. Cosmochim. Acta* **58,** 4739–4750.

Polyakov V. B. and Kharlashina N. N. (1995) The use of heat capacity data to calculate carbon isotope fractionation between graphite, diamond, and carbon dioxide: A new approach. *Geochim. Cosmochim. Acta* **59,** 2561–2572.

Rathmell M. A., Streepey M. M., Essene E. J., and van der Pluijm B. A. (1999) Comparison of garnet-biotite, calcite-graphite, and calcite-dolomite thermometry in the Grenville Orogen; Ontario, Canada. *Contrib. Mineral. Petrol.* **134,** 217–231.

Reeder R. J. (1983) Chrystal chemistry of rhombohedral carbonates. In *Carbonates: Mineralogy and Chemistry* (ed. R. J. Reeder), pp. 1–47. Reviews in Mineralogy 11.

Richards I. J., Labotka T. C., and Gregory R. T. (1996) Contrasting stable isotope behavior between calcite and dolomite marbles, Lone Mountain, Nevada. *Contrib. Mineral. Petrol.* **123,** 202–221.

Richet P., Bottinga Y., and Javoy M. (1977) A review of hydrogen, carbon, nitrogen, oxygen, sulphur, and chlorine stable isotope fractionation among gaseous molecules. *Ann. Rev. Earth Planet. Sci.* **5,** 65–110.

Ross S. D. and Goldsmith J. (1964) Factors affecting the infra-red spectra of planar anions with D_{3h} symmetry—I. Carbonates of the main group and first row transition elements. *Spectrochim. Acta* **20,** 781–784.

Rubinson M. and Clayton R. N. (1969) Carbon-13 fractionation between aragonite and calcite. *Geochim. Cosmochim. Acta* **33,** 997–1002.

Scheele N. and Hoefs J. (1992) Carbon isotope fractionation between calcite, graphite and CO_2: an experimental study. *Contrib. Mineral. Petrol.* **112,** 35–45.

Scheetz B. E. and White W. B. (1977) Vibrational spectra of the alkaline earth double carbonates. *Am. Mineral.* **62,** 36–50.

Schroeder R. R., Weir C. E., and Lippincott E. R. (1962) Lattice frequencies and rotational barriers for inorganic carbonates and nitrates from low temperature infrared spectroscopy. *J. Res. Nat. Bureau Standards A Phys. Chem.* **66A,** 407–434.

Schwarcz H. P. (1966) Oxygen and carbon isotopic fractionation between coexisting metamorphic calcite and dolomite. *J. Geol.* **74,** 38–48.

Shannon R. D. (1976) Revised effective ionic radii and systematic studies of interatomic distances in halides and chalcogenides. *Acta Crystallogr.* **A32,** 751–767.

Sheppard S. M. F. and Schwarcz H. P. (1970) Fractionation of carbon and oxygen isotopes and magnesium between coexisting metamorphic calcite and dolomite. *Contrib. Mineral. Petrol.* **26,** 161–198.

Stolper E. M. and Fine G. J. (1985) The solubility of carbon dioxide in albitic melt. *Mineralogy* **72,** 1071–1085.

Taylor W. R. Green D. H. (1987) The petrogenetic role of methane: Effect on liquidus phase relations and the solubility mechanism of reduced C-H volatiles. In *Magmatic Processes: Physicochemical Principles* (ed. B. O. Mysen), pp. 121–;138. Special Publication 1. Geochemical Society.

Trull T., Pineau F., Bottinga Y., and Javoy M. (1992) CO_2 bubble growth and $^{13}C/^{12}$ C isotopic fractionation in basaltic melt. *Eos* **73 (***no. 14, Suppl.***),** 348.

Turner J. V. (1982) Kinetic fractionation of carbon-13 during calcium carbonate precipitation. *Geochim. Cosmochim. Acta* **46,** 1183–1191.

Urey H. C. and Greiff L. J. (1935) Isotopic exchange equilibria. *J. Am. Chem. Soc.* **57,** 321–327.

Urey H. (1947) The thermodynamic properties of isotopic substances. *J. Chem. Soc. Lond.* 562–581.

Valley J. W. and O'Neil J. R. (1981) $^{13}C/^{12}C$ exchange between calcite and graphite; a possible thermometer in Grenville marbles. *Geochim. Cosmochim. Acta* **45,** 411–419.

Vogel J. C. (1959) Isotopen Trennfaktoren des Kohlenstoffs im Gleichgewichtssystem Kohlendioxyd-Biakarbonat-Karbonat. Ph.D. thesis. Heidelberg University.

Wada H. and Oana S. (1975) Carbon and oxygen isotope studies of graphite bearing carbonates in the Kasuga area, Gifu Prefecture, central Japan. *Geochem. J.* **9,** 149–160.

Table A1. Herzberg's labeling convention.

Frequency	Mode of motion
ν_1	Symmetric stretch
ν_2	Out-of-plane bend
ν_3	Asymmetric stretch
ν_4	In-plane bend

Wada H. and Suzuki K. (1983) Carbon isotopic thermometry calibrated by dolomite-calcite solvus temperatures. *Geochim. Cosmochim. Acta* **47,** 697–706.

Weir C. E. and Lippincott E. R. (1961) Infrared studies of aragonite, calcite, and vaterite type structures in borates, carbonates, and nitrates. *J. Res. Nat. Bureau Standards A Phys. Chem.* **65A,** 173–183.

White W. B. (1974) The carbonate minerals. In *The Infrared Spectra of Minerals*(ed. V. C. Farmer), pp 227–284. Min. Soc. London.

Williams Q., Collerson B., and Knittle E. (1992) Vibrational spectra of magnesite ($MgCO_3$) and calcite-III at high pressures. *Am. Mineral.* **77,** 1158–1165.

Yamamoto A., Shiro Y., and Murata H. (1974) Optically-active vibrations and elastic constants of calcite and aragonite. *Bull. Chem. Soc. Jpn.* **47,** 265–273.

APPENDIX

A1. Vibrations of the Carbonate Ion and the Carbonate Lattice

The vibrational modes of calcite are conventionally described with two $CaCO_3$ units in the primitive cell. As there are 10 atoms per unit cell there will be 30 degrees of vibrational freedom. Twelve of these are taken up by the vibrations of the CO_3^{2-} group (internal modes) and 18 by vibrations of the carbonate group with respect to the cations (external modes). The carbonate ion in carbonates can be expected to exhibit vibrational frequencies that are very similar to those of the free carbonate ion. Following the labeling convention established by Herzberg (1945) these are given in Table A1. Frequencies ν_3, ν_4 are doubly degenerate, which then accounts for 6 degrees of freedom per carbonate ion, i.e., 12 in the carbonate lattice.

Different approaches have been taken in order to determine the effect of isotopic substitution on the vibrational properties and it is of interest to examine how large the differences between different approaches are. For the free carbonate ion Herzberg (1945) developed relationships between the vibrational frequencies and force constants as follows:

$$\lambda_1 = \frac{k_1}{m_o} \tag{A1}$$

$$\lambda_2 = \left(1 + \frac{3 \times m_o}{m_c}\right) \times \frac{k_\Delta}{m_o \times r^2} \tag{A2}$$

$$\lambda_3 + \lambda_4 = \left(1 + \frac{3 \times m_o}{2 \times m_c}\right) \times \left(\frac{k_1}{m_o} + \frac{3 \times k_\delta}{m_o \times r^2}\right) \tag{A3}$$

$$\lambda_3 \times \lambda_4 = 3 \times \left(1 + \frac{3 \times m_o}{m_c}\right) \times \frac{k_1 \times k_\delta}{m_o^2 \times r^2} \tag{A4}$$

The λ's are related to the vibrational frequencies as follows:

$$\lambda_i = \frac{4 \times \pi^2 \times c^2 \times \nu_i^2}{N_o} \tag{A5}$$

where

k_1 = bond stretching force constant
k_Δ = out-of-plane bond bending force constant
k_δ = in-plane bond bending force constant
N_o = Avogadro's number
c = the speed of light
r = the carbon-oxygen bond length
m_c = the mass of the carbon atom
m_o = the mass of the oxygen atom

Using these equations and the observed frequencies, the force constants can be computed. Under the assumption that the force constants are the same for isotopically substituted carbonate ions, the frequencies for the isotopically substituted species can be computed by making the appropriate changes in the masses of the C or O atoms. The computed isotope shift, i.e., the ratio of the $^{13}CO_3^{2-}/^{12}CO_3^{2-}$ frequencies is recorded in Table A2.

A somewhat different treatment of the relationships between vibrational frequencies and the force constants of the carbonate molecule was developed by Heath and Linnett (1948). The relationship for the totally symmetrical vibration is given by:

$$\lambda_1 = (k'_1 + 6 \times A) \times \frac{1}{m_o} \tag{A6}$$

The relationship for the out-of-plane vibration is:

$$\lambda_2 = (k_\beta + 3 \times B') \times \left(\frac{1}{m_o} + \frac{3}{m_c}\right) \tag{A7}$$

The two degenerate planar vibrations follow the relationships:

$$\lambda_3 + \lambda_4 = \left(k'_1 - \frac{3}{4} \times B' + \frac{3}{2} \times A\right) \times \left(\frac{1}{m_o} + \frac{3}{2 \times m_c}\right) + \left[k_\beta + \frac{9}{4} \times B' + \frac{3}{2} \times A\right] \times \left(\frac{1}{m_o} + \frac{3}{2 \times m_c}\right) - (2 \times A - B') \times \frac{9}{4 \times m_c} \tag{A8}$$

and

$$\lambda_3 \times \lambda_4 = \left\{\left(k'_1 - \frac{3}{4} \times B' + \frac{3}{2} \times A\right) \times \left(k_\beta + \frac{9}{4} \times B' + \frac{3}{2} \times A\right) - \frac{9}{16} \times (2 \times A - B')^2\right\} \times \left(\frac{1}{m_o^2} + \frac{3}{m_c \times m_2}\right) \tag{A9}$$

A, B′, k'_1 and k_β are constants. λ is defined as above but it should

Table A2. Frequency shifts for internal modes used in previous studies and this work.

	Chacko et al. (1991)	Golyshev et al. (1981)	Bottinga (1968)	Urey and Greiff (1935)	Urey (1947)	McCrea (1950)	This work: Herzberg (1945)	This work: Heath and Linnett (1948)	Range ‰
ν_1	1	1	1	1	1	1	1	1	0
ν_2	0.968649	0.9686	0.968649	0.968793	0.968747	0.968628	0.968646	0.968646	0.2
ν_3	0.972068	0.9724	0.972425	0.969381	0.970000	0.97700	0.972289	0.972420	7.9
ν_4	0.996475	0.99612	0.996124	0.999300	0.998333	0.998333	0.996253	0.996119	3.2

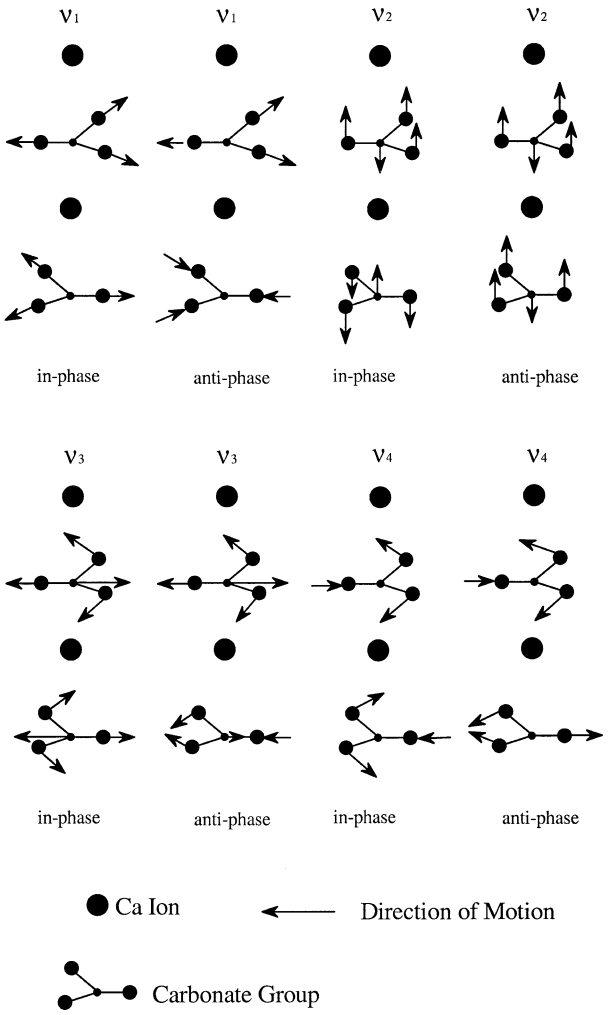

Fig. A1. The internal modes of the carbonate ion in calcite.

be noted that in the paper by Heath and Linnett (1948) λ_2 and λ_3 correspond to λ_3 and λ_4 of Herzberg (1945).

The constants in these equations can be evaluated from the observed vibrational frequencies, and once these are known, the frequency shifts, which occur as the result of isotopic substitution, can be computed. The computed frequency shifts are recorded in Table A2.

Since there are two CO_3^{2-} groups in the unit cell there are two sets of internal vibrations which vibrate either in phase or anti-phase with respect to the center of symmetry (see Fig. A1). Their numerical values are distinct from those of the free carbonate ion because the carbonate group occurs in a crystal lattice. Also, the carbonate groups as a whole will vibrate against the cations in the lattice, producing a set of low-frequency lattice modes, shown in Figure A2. Since five of these modes are doubly degenerate (Table A3), these modes account for 15 degrees of freedom. This leaves 3 degrees of freedom that are attributed to acoustic modes.

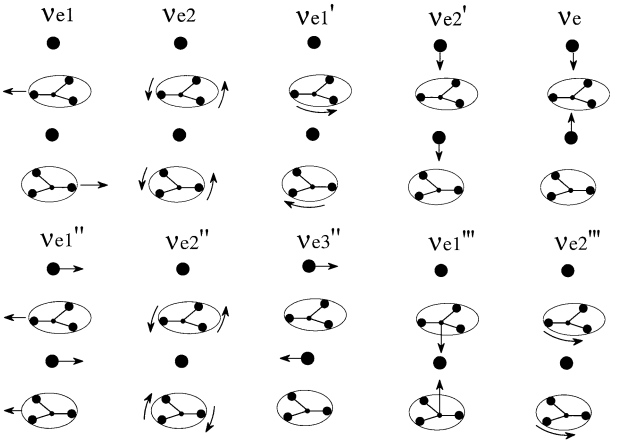

Fig. A2. The lattice modes of the calcite structure.

The notation for the lattice modes has not been as standardized as for the internal modes. In Table A3 the notation of White (1974) of Giulotto and Loinger (1951) and that adopted in this work are shown.

Not all of the external modes have been observed, but Giulotto and Loinger (1951) have developed relationships between the frequencies of the lattice modes and their force constants which permitted them to evaluate unobserved frequencies. The model of Giulotto and Loinger (1951) was used here also to determine the frequency shifts which occur upon isotopic substitution. We define:

$$\omega_i^2 = (\nu e_i \times c \times 2 \times \pi)^2 \tag{A10}$$

where i denotes the *i*th frequency, and the reduced mass is:

$$\mu = \frac{M_p \times M}{M_p + M} \tag{A11}$$

M_p is the mass of the Ca^{2+} ion, and M the mass of the carbonate ion. Four of the force constants involved (c_1, c_2, c_3, c_{13}) can be found from four frequencies by solving simultaneously the relationships (Giulotto and Loinger, 1951) below.

Table A3. Notation for lattice modes.

Giulotto and Loinger notation		White notation			Figure A2
Frequency	Symmetry	Frequency	Symmetry	Degeneracy	
ν	$A_{1u}^{(t)}$	ν_5	A_{1u}	1	νe
ν_1	$E_g^{(t)}$	ν_{13}	E_g	2	νe_1
ν_2	$E_g^{(p)}$	ν_{14}	E_g	2	νe_2
ν_1'	$A_{2u}^{(v)}$	ν_7	A_{2u}	1	$\nu e_1'$
ν_2'	$A_{2u}^{(t)}$	ν_6	A_{2u}	1	$\nu e_2'$
ν_1''	$E_{u(1)}^{(t)}$	ν_8	E_u	2	$\nu e_2''$
ν_2''	$E_u^{(p)}$	ν_{10}	E_u	2	$\nu e_2''$
ν_3''	$E_u^{(v)}$	ν_9	E_u	2	$\nu e_3''$
ν_1'''	$A_{2g}^{(t)}$	ν_{11}	A_{2g}	1	$\nu e_1'''$
ν_2'''	$A_{2g}^{(v)}$	ν_{12}	A_{2g}	1	$\nu e_2'''$

$$\omega_1^2 = \frac{1}{2} \times \left[\frac{2}{m_o} \times c_3 + \frac{3}{M} \times (c_1 + c_2)\right] + \frac{1}{2} \times \sqrt{\left[\frac{2}{m_o} \times c_3 - \frac{3}{M} \times (c_1 + c_2)\right]^2 + 4 \times \left(\frac{\sqrt{3}}{2 \times m_o} \times c_{13}\right) \times \left(\frac{\sqrt{3}}{M} \times c_{13}\right)} \tag{A12}$$

$$\omega_2^2 = \frac{1}{2} \times \left[\frac{2}{m_o} \times c_3 + \frac{3}{M} \times (c_1 + c_2)\right] - \frac{1}{2} \times \sqrt{\left[\frac{2}{m_o} \times c_3 - \frac{3}{M} \times (c_1 + c_2)\right]^2 + 4 \times \left(\frac{\sqrt{3}}{2 \times m_o} \times c_{13}\right) \times \left(\frac{\sqrt{3}}{M} \times c_{13}\right)} \tag{A13}$$

$$\omega'^{2}_{1} = \frac{1}{2}\times\left[\frac{6}{\mu}\times c_3 + \frac{2}{m_o}\times c_1\right] + \frac{1}{2} \times \sqrt{\left(\frac{6}{\mu}\times c_3 - \frac{2}{m_o}\times c_1\right)^2 + 4\times\left(\frac{3}{\mu}\times c_{13}\right)\times\left(\frac{1}{m_o}\times c_{13}\right)} \quad (A14)$$

$$\omega'^{2}_{2} = \frac{1}{2}\times\left[\frac{6}{\mu}\times c_3 + \frac{2}{m_o}\times c_1\right] - \frac{1}{2} \times \sqrt{\left(\frac{6}{\mu}\times c_3 - \frac{2}{m_o}\times c_1\right)^2 + 4\times\left(\frac{3}{\mu}\times c_{13}\right)\times\left(\frac{1}{m_o}\times c_{13}\right)} \quad (A15)$$

A fifth force constant can be found from the frequency ν_2''. For convenience of determining the fifth force constant, c_{34}, the constants C1, C2, and C3 are defined:

$$C1 = \left[\frac{3}{\mu}\times(c_1+c_2) + \frac{3}{M_p}\times(c_1+c_2) + \frac{2}{m_o}\times c_3\right]\times\omega''^{2}_{2} \quad (A16)$$

$$C2 = \frac{3}{\mu}\times(c_1+c_2)\times\frac{3}{M_p}\times(c_1+c_2) + \frac{3}{\mu}\times(c_1+c_2)\times\frac{2}{m_o}\times c_3 + \frac{3}{M_p}\times(c_1+c_2)\times\frac{2}{m_o}\times c_3 - \frac{\mu}{2\times m_o}\times\left(\frac{\sqrt{3}}{\mu}\times c_{13}\right)^2 \quad (A17)$$

$$C3 = \frac{-3}{\mu}\times(c_1+c_2)\times\frac{3}{M_p}\times(c_1+c_2)\times\frac{2}{m_o}\times c_3 + \frac{3}{M_p}\times(c_1+c_2)\times\frac{\mu}{2\times m_o}\times\left(\frac{\sqrt{3}}{\mu}\times c_{13}\right)^2 \quad (A18)$$

With these definitions the fifth force constant can be found from:

$$c_{34} = \sqrt{\frac{C1 - (\omega_2'')^3 - C2\times\omega_2''^2 - C3}{\frac{3}{\mu}\times(c_1+c_2) - 1}\times\frac{2\times m_o}{M_p}\times\frac{M_p^2}{4}} \quad (A19)$$

It should be noted that the approach taken here differs from that of Giulotto and Loinger (1951) who evaluated the force constant from four frequencies and an IR intensity ratio, in that here only vibrational frequencies were used to find the force constants. Once the force constants are known, the frequencies of the lattice modes (see Fig. A2) of the isotopically substituted form of $Ca^{13}CO_3$, can be computed as follows.

$$\nu e = \frac{\sqrt{\omega^2}}{2\times c\times\pi} \quad (A20)$$

where

$$\omega^2 = \frac{6}{M_p}\times c_3 \quad (A21)$$

The frequencies νe_1 and νe_2 are computed from:

$$\nu e_1 = \frac{\sqrt{\omega_1^2}}{2\times c\times\pi} \quad (A22)$$

and

$$\nu e_2 = \frac{\sqrt{\omega_2^2}}{2\times c\times\pi} \quad (A23)$$

where:

$$\omega_1^2 = \frac{\frac{2}{m_o}\times c_3 + \frac{3}{M}\times(c_1+c_2)}{2} + \frac{\sqrt{\left[\frac{2}{m_o}\times c_3 - \frac{3}{M}\times(c_1+c_2)\right]^2 + 4\times\left(\frac{\sqrt{3}}{2\times m_o}\times c_{13}\right)\times\left(\frac{\sqrt{3}}{M}\times c_{13}\right)}}{2} \quad (A24)$$

$$\omega_2^2 = \frac{\frac{2}{m_o}\times c_3 + \frac{3}{M}\times(c_1+c_2)}{2} - \frac{\sqrt{\left[\frac{2}{m_o}\times c_3 - \frac{3}{M}\times(c_1+c_2)\right]^2 + 4\times\left(\frac{\sqrt{3}}{2\times m_o}\times c_{13}\right)\times\left(\frac{\sqrt{3}}{M}\times c_{13}\right)}}{2} \quad (A25)$$

The frequencies $\nu e_1'$ and $\nu e_2'$ are found from:

$$\nu e_1' = \frac{\sqrt{\omega_1'^2}}{2\times c\times\pi} \quad (A26)$$

and

$$\nu e_2' = \frac{\sqrt{\omega_2'^2}}{2\times c\times\pi} \quad (A27)$$

where

$$\omega'^{2}_{1} = \frac{\frac{6}{\mu}\times c_3 + \frac{2}{m_o}\times c_1}{2} + \frac{\sqrt{\left(\frac{6}{\mu}\times c_3 - \frac{2}{m_o}\times c_1\right)^2 + 4\times\left(\frac{3}{\mu}\times c_{13}\right)\times\left(\frac{1}{m_o}\times c_{13}\right)}}{2} \quad (A28)$$

and

$$\omega'^{2}_{2} = \frac{\frac{6}{\mu}\times c_3 + \frac{2}{m_o}\times c_1}{2} - \frac{\sqrt{\left(\frac{6}{\mu}\times c_3 - \frac{2}{m_o}\times c_1\right)^2 + 4\times\left(\frac{3}{\mu}\times c_{13}\right)\times\left(\frac{1}{m_o}\times c_{13}\right)}}{2} \quad (A29)$$

The frequencies $\nu e_1''$, $\nu e_2''$, and $\nu e_3''$ are obtained as the three roots, x_1, x_2, x_3, of the cubic equation:

$$a_3\times x^3 + a_2\times x^2 + a_1\times x + a_o = 0 \quad (A30)$$

$$\nu e''_1 = \frac{\sqrt{x_1}}{2\times c\times\pi} \quad (A31)$$

$$\nu e''_2 = \frac{\sqrt{x_2}}{2\times c\times\pi} \quad (A32)$$

$$\nu e''_3 = \frac{\sqrt{x_3}}{2 \times c \times \pi} \tag{A33}$$

The constants a_0, a_1, a_2, a_3 are defined as follows:

$$a_0 = -\frac{3}{\mu} \times (c_1 + c_2) \times \frac{3}{M_p} \times (c_1 + c_2) \times \frac{2}{m_o} \times c_3 + \frac{3}{\mu} \times (c_1 + c_2) \times \frac{M_p}{2 \times m_o} \times \left(\frac{2}{M_p} \times c_{34}\right)^2 + \frac{3}{M_p} \times (c_1 + c_2) \times \frac{\mu}{2 \times m_o} \times \left(\frac{\sqrt{3}}{\mu} \times c_{13}\right)^2 \tag{A34}$$

$$a_1 = \frac{3}{\mu} \times (c_1 + c_2) \times \frac{3}{M_p} \times (c_1 + c_2) + \frac{3}{\mu} \times (c_1 + c_2) \times \frac{2}{m_o} \times c_3 + \frac{3}{M_p} \times (c_1 + c_2) \times \frac{2}{m_o} \times c_3 - \frac{\mu}{2 \times m_o} \times \left(\frac{\sqrt{3}}{\mu} \times c_{13}\right)^2 - \frac{M_p}{2 \times m_o} \times \left(\frac{2}{M_p} \times c_{34}\right)^2 \tag{A35}$$

$$a_2 = -\left[\frac{3}{\mu} \times (c_1 + c_2) + \frac{3}{M_p} \times (c_1 + c_2) + \frac{2}{m_o} \times c_3\right] \tag{A36}$$

$$a_3 = 1 \tag{A37}$$

The remaining two frequencies, $\nu e'''_1$ and $\nu e'''_2$ can be computed from:

$$\nu e'''_1 = \frac{\sqrt{\omega'''^2_1}}{2 \times c \times \pi} \tag{A38}$$

$$\nu e'''_2 = \frac{\sqrt{\omega'''^2_2}}{2 \times c \times \pi} \tag{A39}$$

where:

$$\omega'''^2_1 = \frac{\frac{6}{M} \times c_3 + \frac{2}{m_o} \times c_1}{2} + \frac{\sqrt{\left(\frac{6}{M} \times c_3 - \frac{2}{m_o} \times c_1\right)^2 + 4 \times \frac{3}{M} \times c_{13} \times \frac{1}{m_o} \times c_{13}}}{2} \tag{A40}$$

and

$$\omega'''^2_1 = \frac{\frac{6}{M} \times c_3 + \frac{2}{m_o} \times c_1}{2} - \frac{\sqrt{\left(\frac{6}{M} \times c_3 - \frac{2}{m_o} \times c_1\right)^2 + 4 \times \frac{3}{M} \times c_{13} \times \frac{1}{m_o} \times c_{13}}}{2} \tag{A41}$$

A2. Estimation of Debye Temperature from Heat Capacity Data

In the computation of the reduced partition function a Debye term is used to account for the isotope effect of those modes that are not represented by specific frequencies. This requires knowledge of a Debye temperature which can be determined from heat capacity data. The heat capacity is made up of contributions from the internal modes plus lattice and acoustic modes of vibration. The contributions from the internal and external modes (when treated explicitly) are computed assuming Einstein oscillators:

$$C_E = \sum_{i=1}^{i=n} \frac{3 \times N \times k \times \left(\frac{\theta_{E_i}}{T}\right)^2 \times e^{\frac{\theta_{E_i}}{T}}}{\left(e^{\frac{\theta_{E_i}}{T}} - 1\right)^2} \tag{A42}$$

where

h = Planck's constant

k = Boltzmann's constant

N = Avogadro's number

T = absolute temperature

$$\theta_{E_i} = \frac{h \times \nu_i}{k}$$

n = the number of frequencies, considering each j times degenerate frequency j times

ν_i = the i^{th} frequency

A unit cell of $CaCO_3$ of 10 atoms is considered which leads to 30 degrees of freedom 12 of them are taken up by the internal modes which leaves 18 to be assigned to lattice and acoustic modes. Ten lattice modes are computed using the method of Giulotto and Loinger (1951), 5 of them are doubly degenerate, (i.e., n = 27). This leaves 3 acoustic modes which are approximated by a Debye oscillator as follows:

$$C_D = 9 \times N \times k \times \left(\frac{T}{\theta_D}\right)^3 \times \int_0^{\frac{\theta_D}{T}} \frac{x^4 \times e^x}{(e^x - 1)^2} dx \tag{A43}$$

where θ_D is the Debye temperature. The sum of the two contributions to the heat capacity is computed from:

$$C_v = C_E + \frac{30 - n}{30} \times C_D \tag{A44}$$

In those instances in which only the internal frequencies were considered, the lattice modes and acoustic modes were lumped in the Debye term; in this case n = 12. Assuming a value for θ_D, the heat capacity was computed according to Eqn. A44 and for temperatures below 298 K the sum of the mean squared deviation between the computed and observed heat capacity was determined. By trial and error θ_D was chosen to minimize this sum.

A3. Computation of the Reduced Partition Functions

The reduced partition function is calculated for a unit cell containing two molecules of $CaCO_3$ (30 degrees of freedom). There are 10 optical and librational modes, five of which are doubly degenerate (15 modes), and two acoustic modes one of which is degenerate (3 modes) which leads to 18 external modes. There are 4 internal modes two of which are doubly degenerate, leading to 6 internal modes per carbonate group and since there are two carbonate groups 12 internal modes are present. Two atoms are exchanged. The frequencies of the isotopically substituted unit cell the and isotope shifts were computed using the model of Heath and Linnett (1948) when only the internal modes were considered explicitly, in addition, the Giulotto and Loinger (1951) model was used when both internal and external modes were treated explicitly. The observed frequencies were used to compute the portion of the heat capacity attributable to them. The remainder of the heat capacity was fitted up to 298 K by choosing a Debye contribution for 3 acoustic frequencies and selecting a Debye temperature, by trial and error, such that the best fit up to T = 298 K was obtained.

The reduced partition function is thus made up of three components and was computed (see Becker, 1971) from:

$$\ln(\beta) = 2 \times \sum_{i=1}^{6} \left\{ \left(\frac{h \times c}{k \times T}\right) \times \frac{1}{2} \times (\nu il_i - \nu ih_i) + \ln\left(\frac{1 - e^{\frac{-h \times c}{k \times T} \times \nu il_i}}{1 - e^{\frac{-h \times c}{k \times T} \times \nu ih_i}}\right) \right\} + \sum_{i=1}^{15} \left\{ \left(\frac{h \times c}{k \times T}\right) \times \frac{1}{2} \right.$$

Table A4. Summary of wave numbers (cm^{-1}) of internal modes used in previous studies.

	Chacko et al. (1991)	Golyshev et al. (1981)	Bottinga (1968)	Urey and Greiff (1935)	Urey (1947)	McCrea (1950)
ν_1	1070	1070	1070	1087	1087	1086
ν_2	881	855	881	878	878	879
ν_3	1460	1460	1460	1437	1437	1434
ν_4	712	712	712	712	714	712

$$\times (\nu el_i - \nu eh_i) + \ln\left(\frac{1 - e^{\frac{-h\times c}{k\times T}\times \nu el_i}}{1 - e^{\frac{-h\times c}{k\times T}\times \nu eh_i}}\right) + 3 \times \ln\left(\frac{1 - e^{\frac{-\theta 1}{T}}}{1 - e^{\frac{-\theta h}{T}}}\right) + \frac{3}{2} \times \frac{\theta 1 - \theta h}{T} - \frac{1}{20} \times \frac{\theta 1^2 - \theta h^2}{T^2} + \frac{3 \times 2}{2} \times \ln\left(\frac{m_{12}}{m_{13}}\right) \quad (A.45)$$

where

νil = are the internal vibrational modes of the ^{12}C substituted unit cell

νih = are the internal vibrational modes of the ^{13}C substituted unit cell

νel = are the external vibrational modes of the ^{12}C substituted unit cell

νeh = are the external vibrational modes of the ^{13}C substituted unit cell

θl = the Debye temperature evaluated from fitting the low temperature heat capacity data to the heat capacity model

θh= IE*θl, where IE = isotope effect evaluated by forcing the fractionation to be zero at infinite temperatures

m_{12} = mass of the ^{12}C atom

m_{13} = mass of the ^{13}C atom

The first term represents the summation over the internal modes of the two carbonate groups, the second term the summation over the external mode, the third term the modes represented by the Debye term (one such term for every three modes) and the last the partition function ratio for the monatomic C gas. Two carbon atoms are exchanged. To find the reduced partition function for the single C atom exchange the value for ln (β) computed from the equation above is divide by two.

When only one carbonate molecule and only the internal modes (6) are considered and all other modes (9) are lumped in to the Debye term the expression simplifies to:

$$\ln(\beta) = \sum_{i=1}^{6}\left\{\left(\frac{h \times c}{k \times T}\right) \times \frac{1}{2} \times (\nu il_i - \nu ih_i) + \ln\left(\frac{1 - e^{\frac{-h\times c}{k\times T}\times \nu il_i}}{1 - e^{\frac{-h\times c}{k\times T}\times \nu ih_i}}\right)\right\} + 3 \times 3 \times \ln\left(\frac{1 - e^{\frac{-\theta 1}{T}}}{1 - e^{\frac{-\theta h}{T}}}\right) + \frac{3 \times 3}{2} \times \frac{\theta 1 - \theta h}{T} - \frac{3}{20} \times \frac{\theta 1^2 - \theta h^2}{T^2} + \frac{3}{2} \times \ln\left(\frac{m_{12}}{m_{13}}\right) \quad (A46)$$

A4. Examination of Vibrational Frequencies and Their Isotope Shift Used in Earlier Studies

Several of the earlier computations of reduced partition function for calcite have considered only the internal modes (Urey and Greiff, 1935; Urey, 1947; McCrea, 1950; Chacko et al., 1991), while Bottinga (1968) and Golyshev et al. (1981) have included also external modes. The frequencies used in the earlier publications are summarized in Table A4, and it is apparent, in particular in the case of ν_3, that there is a significant range in the wave numbers that have been selected.

An overview of the published frequencies is provided in Figure A3. A significant range of values has been reported for individual frequencies. The values used in the previous computations of Bottinga (1968), Golyshev et al. (1981) and Chacko et al. (1991) have been indicated and it is evident that for ν_1, ν_2, and ν_3 they lie at the extremes of the distribution of wave numbers that have been determined.

Because the value of the assumed frequencies can have a significant effect on the computed reduced partition function, the sensitivity of the computations to the choice of wave number was investigated. The effect of different assumptions about the νs was tested as follows. The computations of 1000 ln K by Chacko et al. (1991) could be duplicated to within less than 0.1 with the algorithm developed for present work, using the frequencies and frequency shifts cited by Chacko et al. (1991) assuming a Debye temperature of 409 K and an isotope effect of 0.997283 for it. Chacko et al. (1991) do not state the Debye temperature value; however, a temperature of 400 K for calcite as well as aragonite was quoted by Rubinson and Clayton (1969) and it is likely that Chacko et al. (1991) used this value. Keeping all other inputs identical one frequency was changed at a time and the change in 1000 ln β at 300 K was noted; with increasing temperature these changes decline.

The frequency ν_1 has no effect on the computed reduced partition function. The effect of the choice of ν_2 is demonstrated in Figure A4. Using the frequency which has been reported most frequently, rather than that chosen by Chacko et al. (1991) and Bottinga (1968), lowers the reduced partition function computed by Chacko et al. (1991) by about 0.3‰.

The ν_3 values, used by Bottinga (1968) and Chacko et al. (1991), are quoted as having been taken from the work of Schroeder et al. (1962). Because the value for ν_3 used in these computations differs significantly from the value used by Urey (1947) and McCrea (1950) (see Table A4), and the range of values reported in the review of IR calcite spectra by Gadsden (1975) (1435 to 1410 cm^{-1}), the original publication of Schroeder et al. (1962) was consulted. Table 5 of this publication lists frequencies for ν_1 (1070 cm^{-1}), ν_2 (881 cm^{-1}), ν_4 (712 cm^{-1})

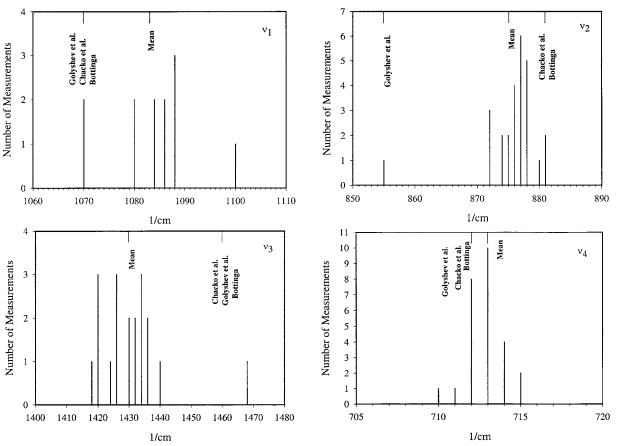

Fig. A3. Compilation of data for internal vibrational modes of calcite, for sources of data see Table 1.

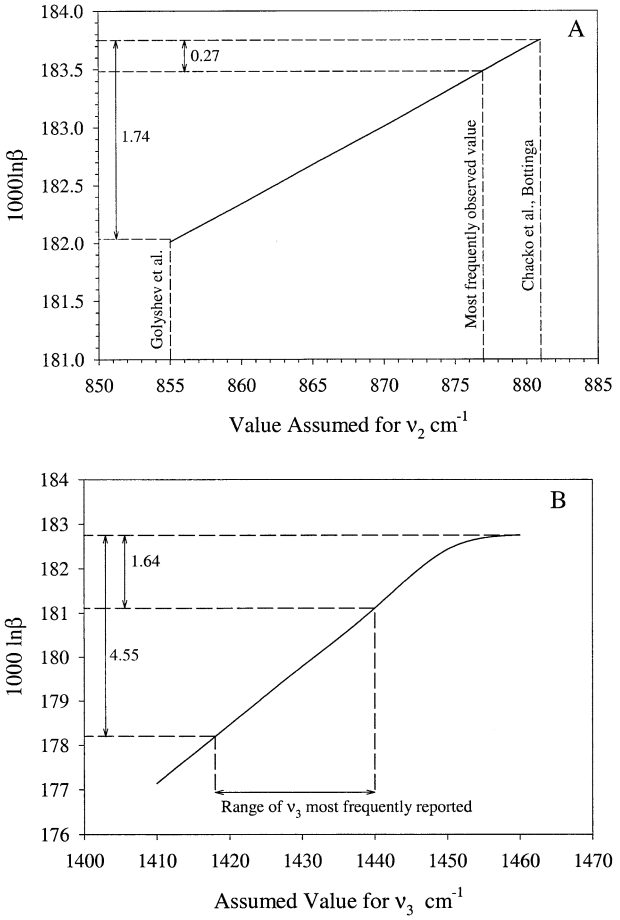

Fig. A4. Effect of the choice of vibrational frequencies ν_2 and ν_3 on the size of the reduced partition function of calcite at 300 K.

but none for ν_3. The authors comment on the determination of ν_3 as follows "ν_3 is always observed but with such great intensity that it is not possible to determine whether it is a single or multiple band or even to locate its position with reliability." This explains the absence of a value for this frequency in table 5 of Schroeder et al. (1962). The source of the specific value for ν_3 used in the computations by Bottinga (1968) and Chacko et al. (1991) is hence unclear. There is only one measurement of ν_3 (1467 cm^{-1}), reported in the publications examined in conjunction with this work (Ross and Goldmith, 1964) that is in the general vicinity of the value used for the earlier computations. Neither Golyshev et al. (1981) nor Chacko et al. (1991) comment on why they selected for this vibration a frequency number that differs considerably from those used by Urey (1947) and McCrea (1950) and the majority of the measured values. Bottinga (1968), who considered frequency measurements from several authors, comments, concerning the selection of frequencies, "Calculations were carried out using both the set quoted by Hexter (1958) (ν_3 = 1432) and that by Schroeder et al. (ν_3 = 1460). The latter set gave slightly better results (i.e., match to the low temperature experimental work), and the calculations reported in this paper have been done with these frequencies." Bottinga (1968) does not state what his understanding (‰ difference) of "slight" is. As it turns out the assumption made about ν_3 has a very significant effect on the outcome of the computation of the reduced partition function of calcite (see also Rubinson and Clayton, 1969).

Figure A4 also demonstrates how 1000 ln β (300 K) changes with varying assumptions about ν_3, and indicates that at ambient temperatures the reduced partition function for calcite is probably by several permil lower than the earlier computations indicate. The computations of Bottinga (1968) were duplicated. Keeping all parameters constant, except changing ν_3 to the value assumed by Urey, this reduces 1000 ln K by about 4‰ at 300 K. The same result was obtained when the computations of Golyshev et al. (1981) and Chacko et al. (1991) were duplicated and this change in ν_3 was made.

The range of wave numbers reported for frequency ν_4 is much more restricted and the value used in the earlier computations falls within one wave number of the most frequently cited value.

The choice of values for ν_2 and ν_3 at the extremes of the observed frequency distributions leads to values of 1000 ln β for calcite that are systematically higher compared to results that are obtained when values more central to the ν distributions are used. Combining the effects of ν_2 and ν_3, the differences at 300 K can be expected to be on the order of 4‰ or larger.

The computations of the shifts in vibrational frequency which occur when ^{13}C is substituted for ^{12}C in the mineral lattice require a model for the vibrations. The frequency shifts for the internal modes used by different authors vary significantly (up to 8‰) depending on the frequency (see Table A2). Computations on the isotope fractionation behavior of the carbonate were first reported by Urey and Greiff (1935). The details of the computation of the frequency shifts were not given. The authors state "Fundamental frequencies $^{12}CO_3$ estimated for us by Dr. Jennie Rosenthal. Frequencies of isotopic $^{13}CO_3$ calculated in

Table A5. Summary of wave numbers of external modes for calcite used in previous studies and this work.[a]

White (1974)	Guilotto and Loinger (1951)				Bottinga (1968)		This work	
		Wave number (cm^{-1})						
Notation	Notation	Observed	Computed	Deg.	Wave number (cm^{-1})	Frequency shift	Wave number (cm^{-1})	Frequency shift
v5	v	295		1	294.6	1.0000	294	1
v6	v2′	106	106	1	106.1	1.0000	106	0.999695
v7	v1′	357	397	1	397.2	0.9970	397	0.997080
v8	v1″	330	344	2	345.3	0.9988	342	0.998946
v9	v3″	182	260	2	256.5	0.9984	259	0.998034
v10	v2″	106	106	2	110.9	0.9973	118	0.999721
v11	v1‴		269	1	269.1	0.9937	269	0.993715
v12	v2‴		99	1	99.1	0.9980	99	0.998014
v13	v1	282	282	2	228.2	0.9989	282	0.998903
v14	v2		155	2	155.1	0.9929	155	0.992831

[a] Deg. = Degeneracy. For the computations of the four force constants the wave numbers v1, v2, v1′, v2′, v2″ were assumed, the remainder of the frequencies were computed based on the model of Giulotto and Loinger (1951).

accordance with relationships she has derived." The shifts used by Urey and Greiff (1935) are given in Table A2. The results of new isotope effect computations were reported by Urey (1947) who, concerning the isotope shifts, refer to the paper by Urey and Greiff (1935), but actually use a different set of shifts (see Table A2). Subsequently McCrea (1950) carried out further computations using the frequencies cited in Table A4 and frequency shifts given in Table A2, which agree, in part, with those of Urey (1947). McCrea does not give the details of his frequency shift computations. More recent computations have been based on the vibrational models for the carbonate group by Heath and Linnett (1948). Herzberg (1945) had reported earlier relationships between the internal vibrational frequencies of planar XY_3 molecules and their force constants, which permit the computation of frequency shifts. For the internal frequencies of calcite, used in this study, results based on the equations of Herzberg (1945) and those of Heath and Linnett (1948) were compared. The difference between the frequency shifts computed by the two approached was less than 0.13‰. The equations of Heath and Linnett (1948) were used throughout the present computations.

The frequency shifts of Chacko et al. (1991) are slightly different from those used by Golyshev et al. (1981) and Bottinga (1968). Chacko et al. (1991) note that although the same equations were used by them as by Bottinga (1968) a slight, but significant, difference is found. No explanation for the cause of the difference was offered. The frequency shift factors computed by the algorithm used in this work for the frequencies assumed by Chacko et al. (1991), Golyshev et al. (1981) and Bottinga (1968) match those of the latter two sets of authors but not those of Chacko et al. (1991). Apparently the approach to determine the frequency shifts used by Chacko et al. (1991) differs from those documented in the literature.

At 300 K the value of 1000 ln β found by Chacko et al. (1991) is reduced from 183.75 to 182.59, i.e., by 1.16‰ if the frequency shift factors of Bottinga (1968), Golyshev et al. (1981) or those computed in this study are used. Combining the effects of frequency choice and frequency shift leads to the conclusion that at 300 K there will be a difference of over 5‰ between the results of Chacko et al. (1991) and computations based on more representative IR frequencies, and the frequency shift factors that are confirmed by three independent studies.

The last parameter that has an effect on the computations is the assumed Debye temperature. The temperature assumed by Chacko et al. (1991) was not stated, however, it is probably close to 400 K, the value assumed by Rubinson and Clayton (1969). In the present work the heat capacity data were fitted, after accounting for the contributions of the internal vibrations, with a Debye function. The sum of squares for the deviations of the observations form this function was then computed. The Debye temperature was chosen so that the sum of squares (ssq) was minimized. A minimum ssq = 6.4 was found for θ_D = 369, for a θ_D = 400 it was slightly larger (ssq = 11.8). The effect of changing the assumed Debye temperature from 409 to 369 was tested. At 300 K the value of 1000lnK was reduced by a further 0.4‰.

The combined effects of choice of frequencies, frequency shifts and Debye temperature will hence lead to a lowering of the partition function reported by Chacko et al. (1991) by about 5.5‰ at 300 K, at higher temperatures this shift will be smaller.